Higher order corrections in Higgs boson pair production within and beyond the SM

Gudrun Heinrich
Max Planck Institute for Physics, Munich

tourism-bw.com

KIT-NEP, October 8, 2019

MAX-PLANCK-GESELLSCHAFT

cost
EUROPEAN COOPERATION IN SCIENCE & TECHNOLOGY

Max-Planck-Institut für Physik
(Werner-Heisenberg-Institut)

Outline

- Combination of full NLO with NNLO_approx
- Combination of full NLO with high energy expansion
- QCD corrections to non-linear EFT description of Higgs boson pair production
- Implementation in POWHEG, parton shower effects
- Shape analysis to improve constraints on anomalous couplings

based on/in collaboration with

1803.02463 Grazzini, GH, Jones, Kallweit, Kerner, Lindert, Mazzitelli

1806.05162 Buchalla, Capozi, Celis, GH, Scyboz

1903.08137 GH, Jones, Kerner, Luisoni, Scyboz

1907.06408 Davies, GH, Jones, Kerner, Mishima, Steinhauser, Wellmann

1908.08923 Capozi, GH

Higgs boson pair production

Higgs trilinear coupling:

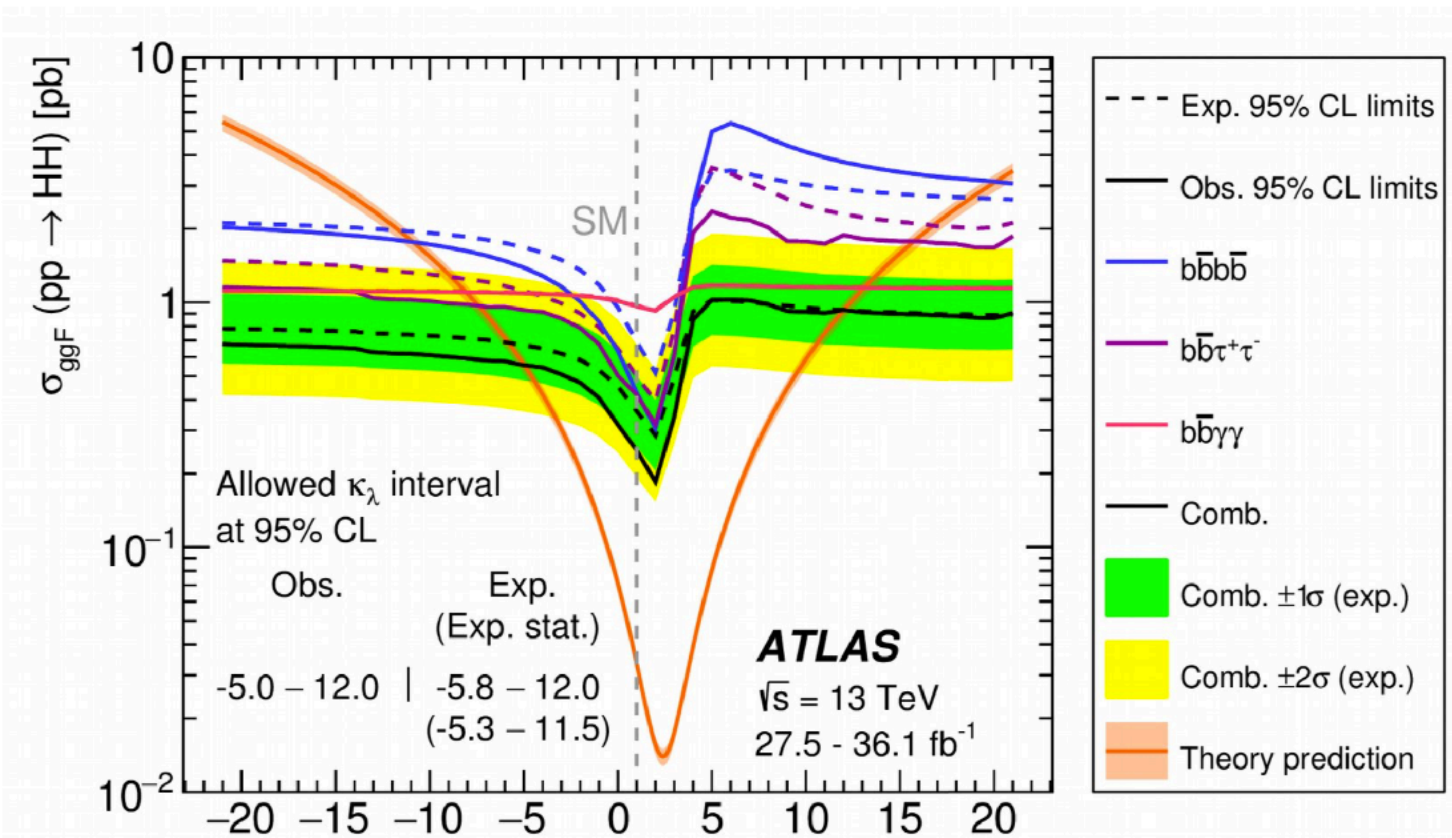

1906.02025

$$-5.0 \leq \lambda/\lambda_{\rm SM} \leq 12.0 \quad \text{(95\% CL)}$$

$$\sigma^{HH}_{\max} = 6.9 \times \sigma_{SM}$$

these limits rely on theory predictions

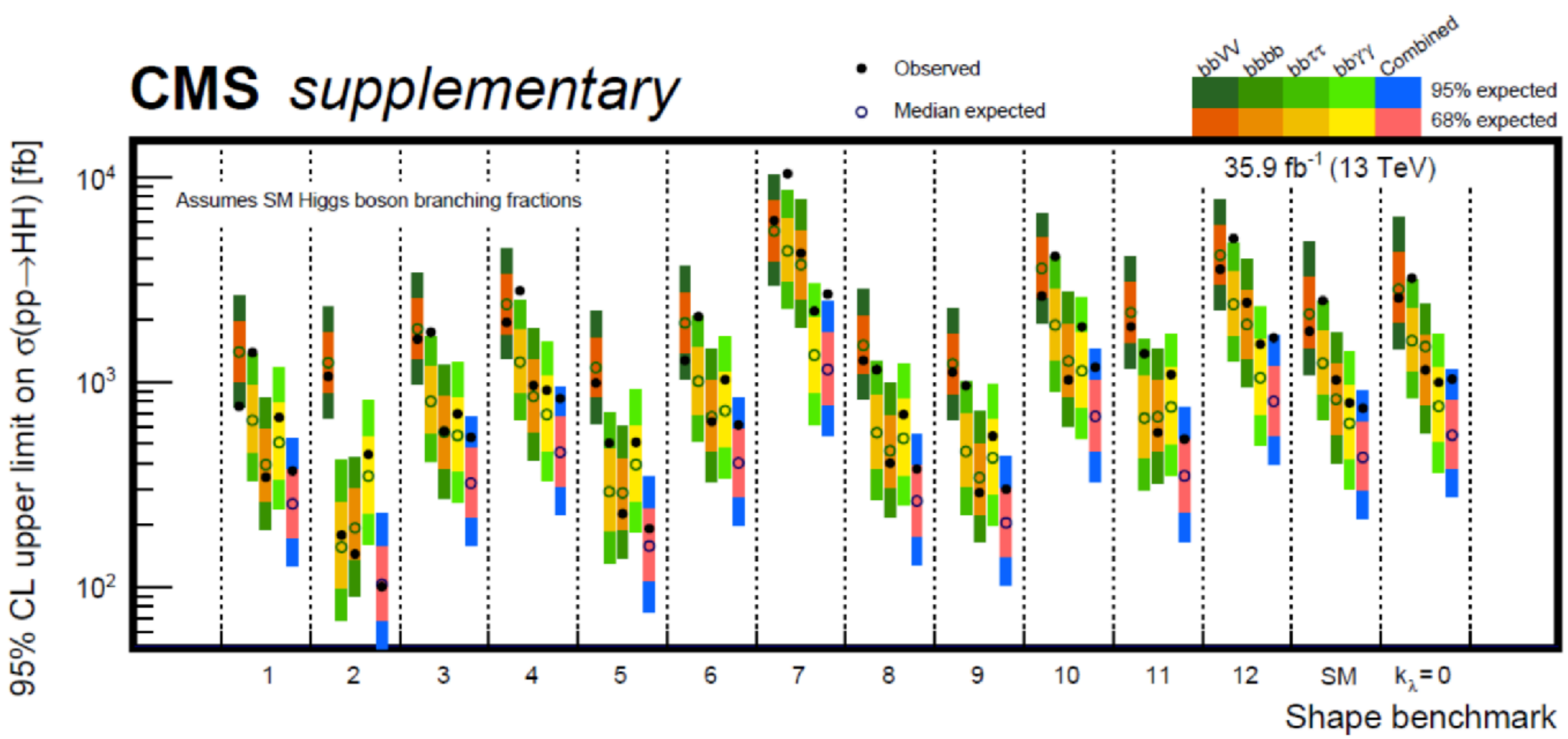

1811.09689

Higgs boson pair production in gluon fusion

approximations:

- $m_t \to \infty$ limit (HTL):

sometimes also called HEFT
("Higgs Effective Field Theory")

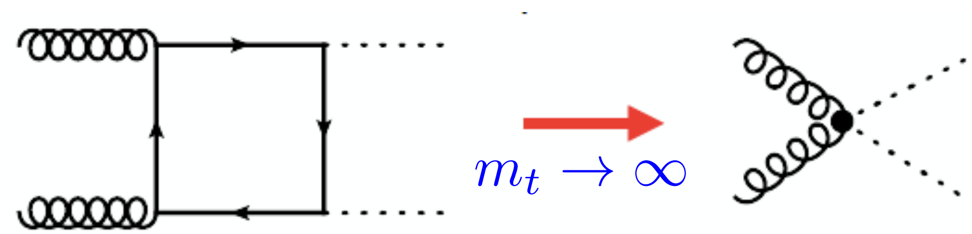

Leading Order (LO)

Glover, van der Bij '88

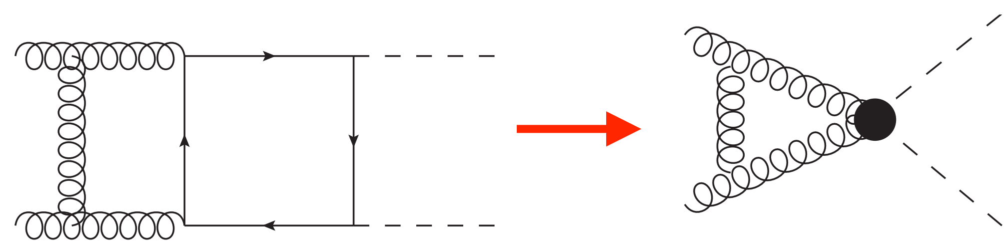

Next-to-Leading Order (NLO)

- Born-improved HTL: Dawson, Dittmaier, Spira '98

$$d\sigma^{\rm NLO}_{m_t\to\infty} \times \frac{d\sigma^{\rm LO}(m_t)}{d\sigma^{\rm LO}_{m_t\to\infty}}$$

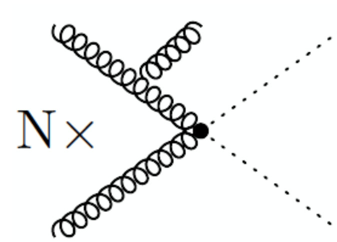

NLO real

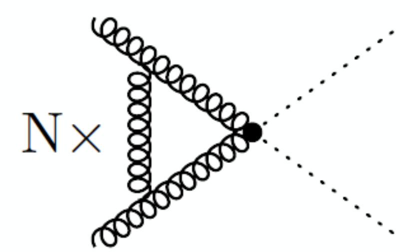

NLO virtual

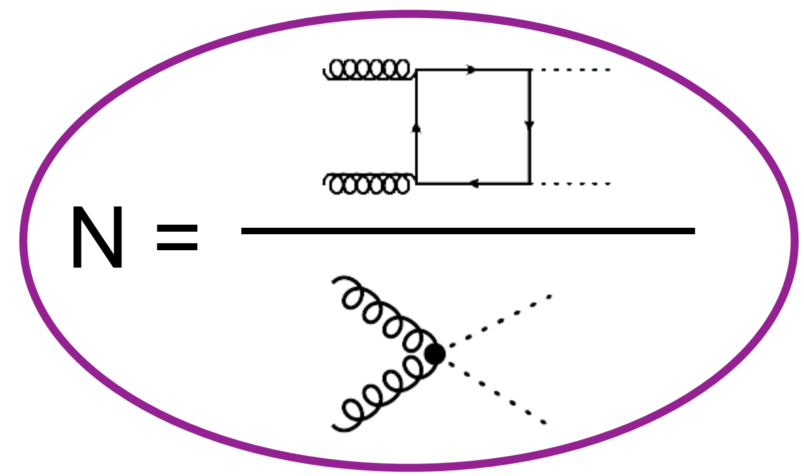

- FTapprox: Maltoni, Vryonidou, Zaro '14

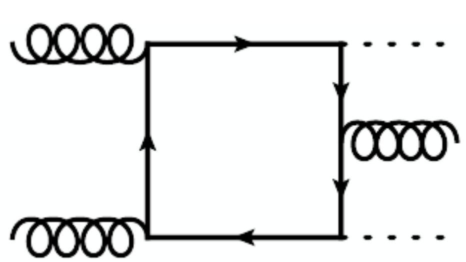

NLO real:
full m_t-dependence

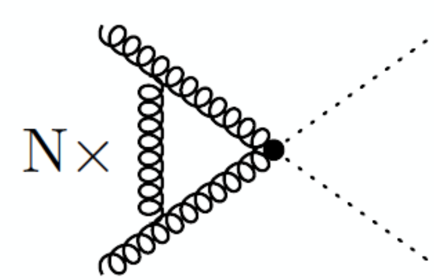

NLO virtual:
Born-improved HTL

Higgs boson pair production in gluon fusion

approximations

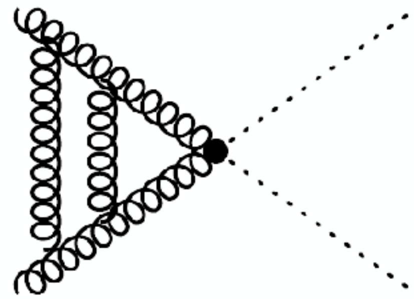

- total cross section NNLO in $m_t \to \infty$ limit De Florian, Mazzitelli '13
- including all matching coefficients Grigo, Melnikov, Steinhauser '14
- supplemented with $1/m_t$ expansion Grigo, Hoff, Steinhauser '15
- soft gluon resummation NNLL Shao, Li, Li, Wang '13; De Florian, Mazzitelli '15
- differential NNLO De Florian, Grazzini, Hanga, Kallweit, Lindert, Maierhöfer, Mazzitelli, Rathlev '16
- NNLL soft gluon resummation on top of NNLO_approx De Florian, Mazzitelli '18
- threshold + $1/m_t$ expansion Gröber, Maier, Rauh '17
- expansion in $p_T^2 + m_h^2$ Bonciani, Degrassi, Giardino, Gröber '18
- high energy expansion Davies, Mishima, Steinhauser, Wellmann '18, '19; Mishima '18
- partial N^3LO $m_t \to \infty$ 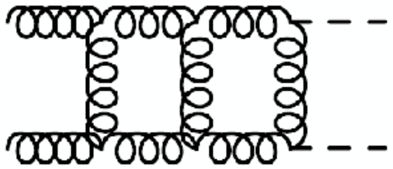 Banerjee, Borowka, Dhani, Gehrmann, Ravindran '18
- (partial) NLO EW corrections Borowka, Duhr, Maltoni, Pagani, Shivaji, Zhao '18
- contribution to real-virtual NNLO 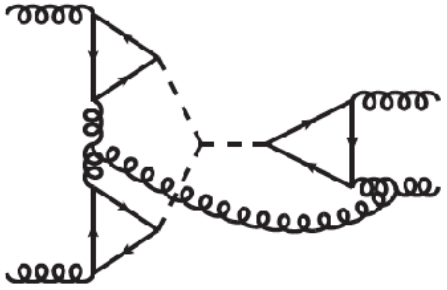 Davies, Herren, Mishima, Steinhauser '19

Higgs boson pair production at full NLO

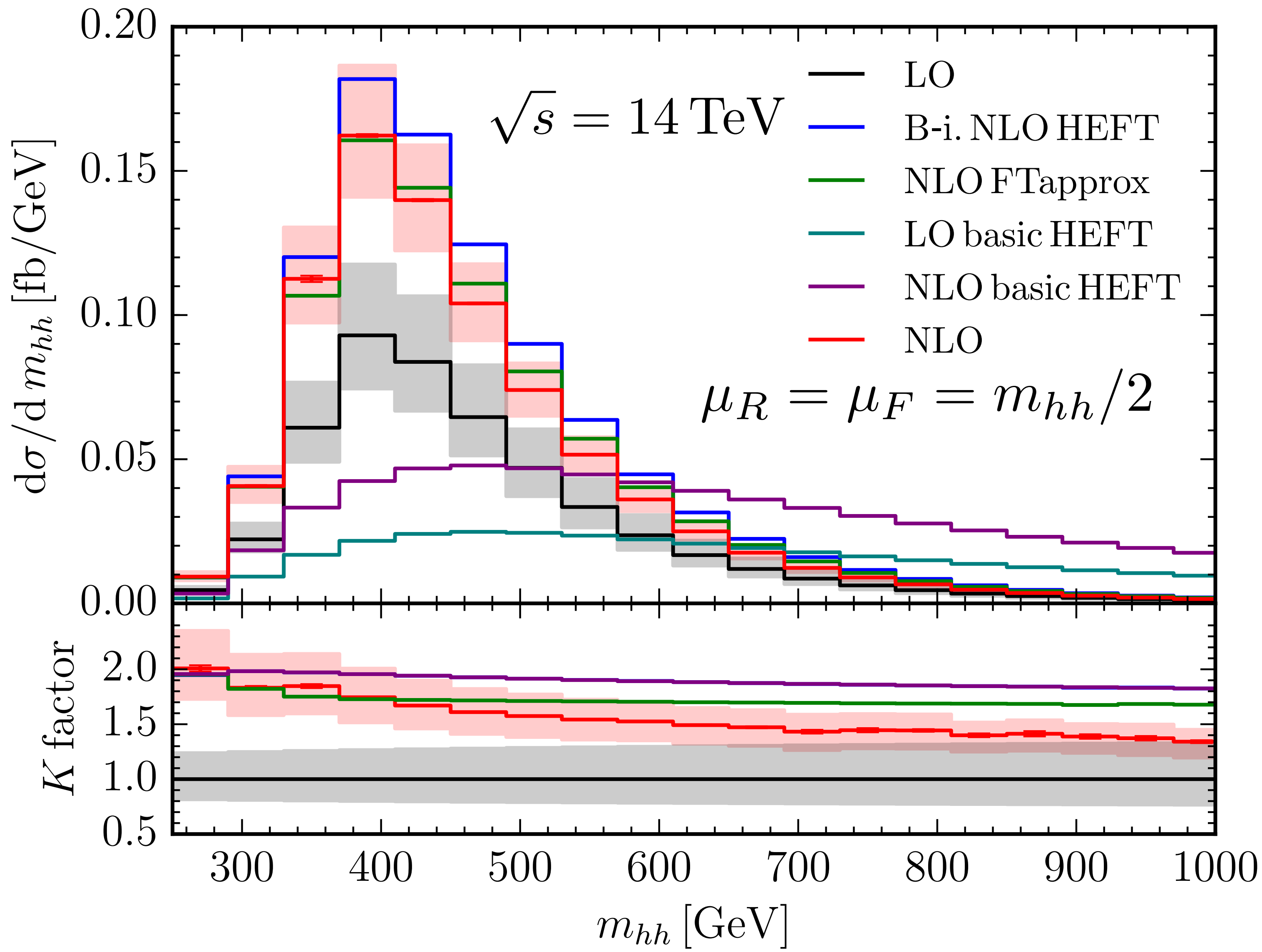

Borowka, Greiner, GH, Jones, Kerner, Schlenk, Schubert, Zirke '16

Baglio, Campanario, Glaus, Mühlleitner, Spira, Streicher '18

$$m_{hh}^2 = (p_{h_1} + p_{h_2})^2$$

at large invariant masses m_{hh} :

Born-improved NLO HEFT 50% too large,

FTapprox ~ 40% too large

top quark loops can be resolved at large energies →

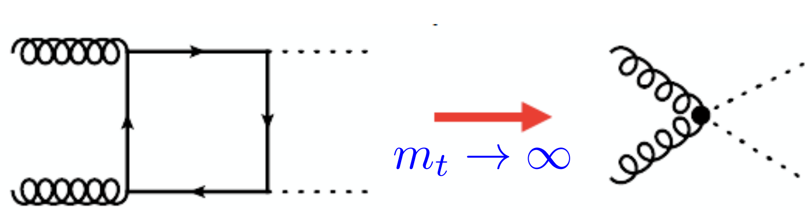

not a good approximation for $m_{hh} \gtrsim 2m_t$

Promote to NNLO_approx

Grazzini, GH, Jones, Kallweit, Kerner, Lindert, Mazzitelli '18

Technical ingredients

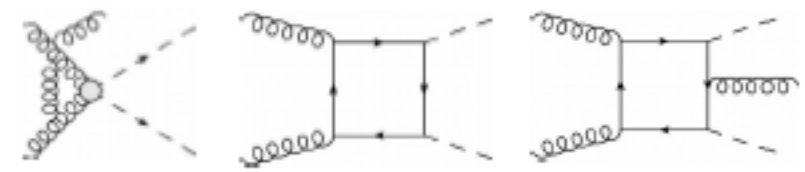

Tree-level and one-loop amplitudes (HEFT and full-M_t) → OpenLoops
[Cascioli, Lindert, Maierhofer, Pozzorini]

Full NLO (two-loop) virtual corrections → two dimensional grid + interpolation
[Borowka, Greiner, Heinrich, Jones, Kerner, Schlenk, Zirke, '16]

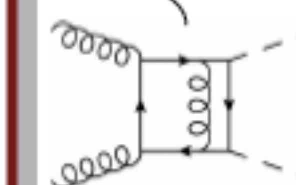

Analytical results for NNLO two-loop corrections in the HEFT
[de Florian, JM, '13]

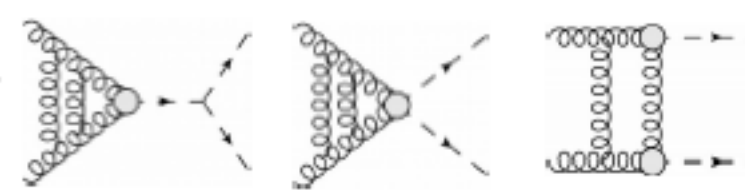

NNLO subtraction formalism: q_T-subtraction
[Catani, Grazzini, '07]

Implementation based on public code MATRIX
[Kallweit, Grazzini, Wiesemann, '17]

NNLO_approx

three approximations:

- NLO-improved NNLO HEFT $\boxed{\text{NNLO}_{\text{NLO-i}}}$

$$\frac{d\sigma^{\text{NLO}-\text{i.NNLO HEFT}}}{dm_{hh}} = \frac{d\sigma_{\text{NLO}}}{dm_{hh}} \times \frac{d\sigma^{\text{HEFT}}_{\text{NNLO}}/dm_{hh}}{d\sigma^{\text{HEFT}}_{\text{NLO}}/dm_{hh}}$$

bin-by-bin rescaling at observable level by NNLO HEFT K-factor

- Born-projected $\boxed{\text{NNLO}_{\text{B-proj}}}$

reweight each NNLO event by the ratio $\text{Born}^{\text{full}}/\text{Born}^{\text{HEFT}}$

different final state multiplicities in single/double real part ⟶ need projection (not unique)

use qT recoil method Catani, De Florian, Ferrera, Grazzini '15

- "approximate Full Theory" $\boxed{\text{NNLO}_{\text{FTapprox}}}$

$\mathcal{O}(\alpha_s^4)$ part: at n-loops in HEFT, X=2-n extra partons: reweight $\mathcal{A}^{(n)}_{\text{HEFT}}(ij \to HH + X)$

with $\mathcal{R}(ij \to HH + X) = \dfrac{\mathcal{A}^{\text{Born}}_{\text{Full}}(ij \to HH + X)}{\mathcal{A}^{(0)}_{\text{HEFT}}(ij \to HH + X)}$

NNLO_approx: mhh

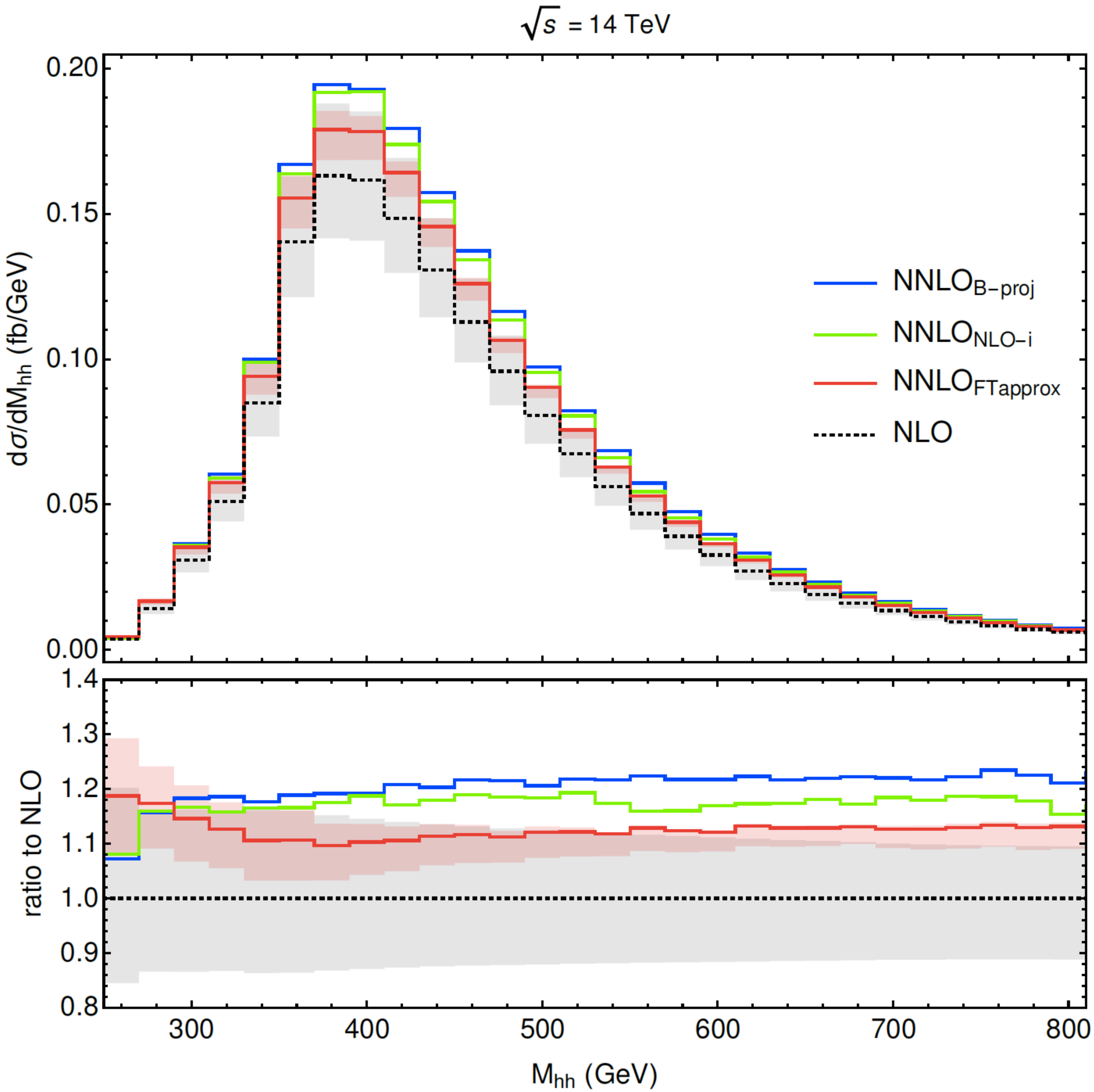

NNLO_FTapprox:

mostly overlaps with NLO uncertainty band

larger corrections at production threshold

scale uncertainties much reduced

NNLO_approx: pT,hh

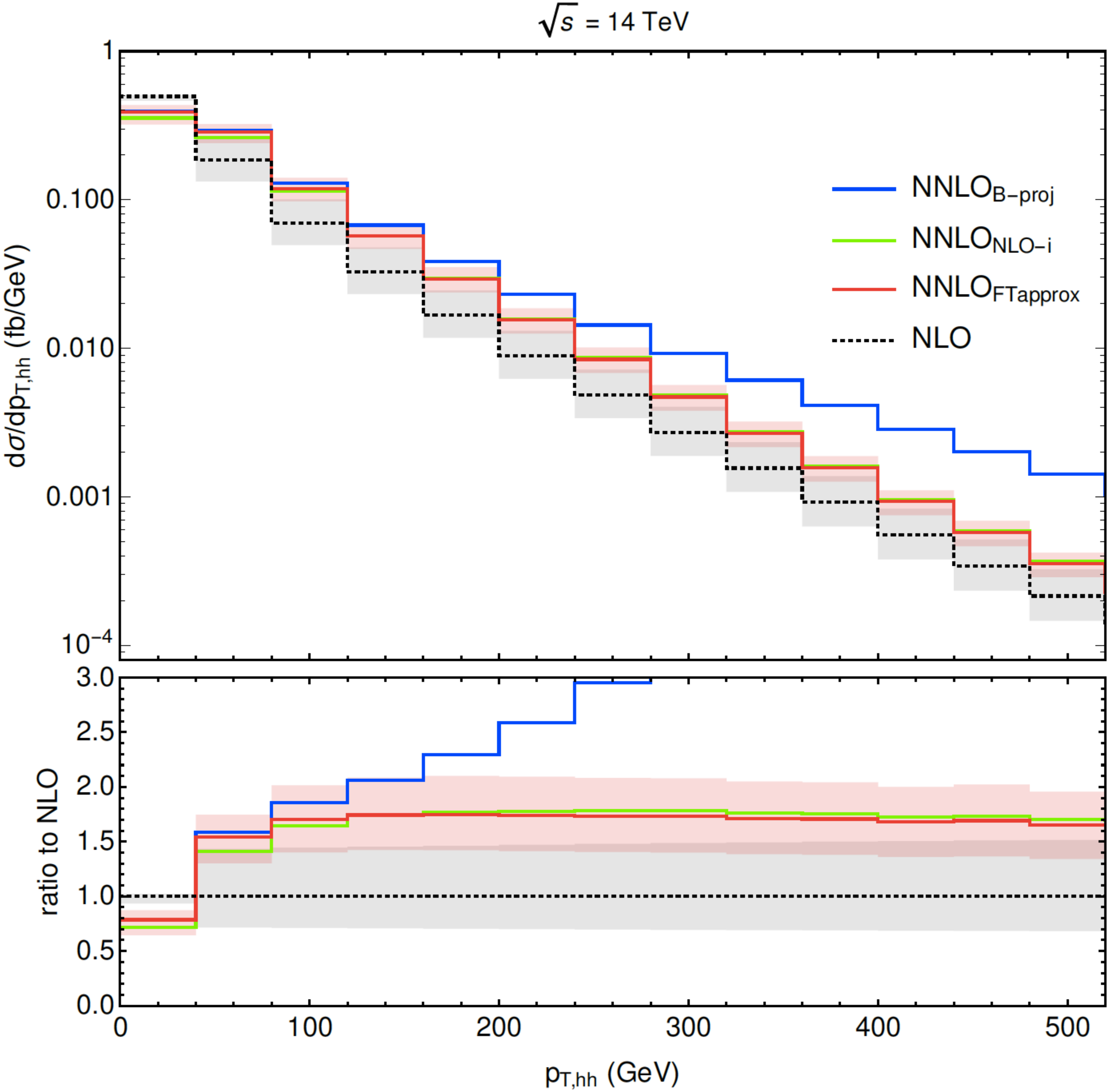

NLO is first non-trivial order for $p_{T,hh}$

→ larger corrections and uncertainties than for m_{hh}

similar pattern as at NLO:

Born-projected has wrong scaling behaviour in the tail

NLO + high energy expansion

high energy limit: $m_h^2 < m_t^2 \ll s, |t|, |u|$

expansion of form factors for $gg \to HH$

Davies, Mishima, Steinhauser, Wellmann '18, '19; Mishima '18

combination with Padé approximants for finite virtual part

$$\mathcal{V}_{\rm fin}^N = \frac{a_0 + a_1 x + \ldots + a_n x^n}{1 + b_1 x + \ldots + b_m x^m} \equiv [n/m](x) \quad (m_t^{2k} \to x\, m_t^{2k})$$

improves convergence

Padé [8/8](x)

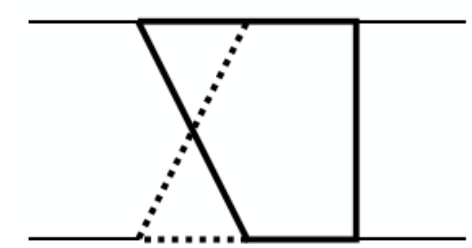

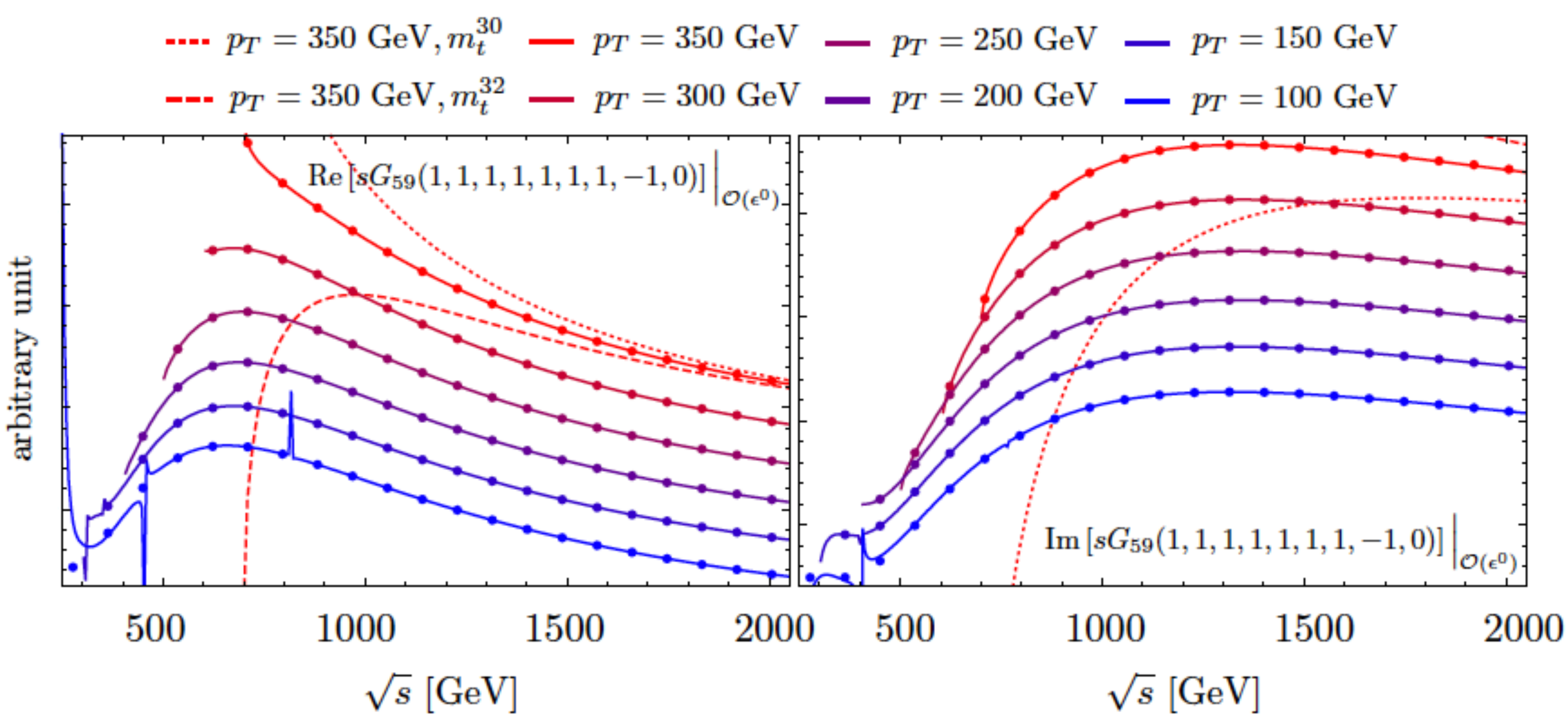

dashed: high energy expansion

solid lines: Padé improved

dots: pySecDec

NLO + high energy expansion

high energy expansion: large uncertainties for $\sqrt{s} \lesssim 800\,\mathrm{GeV}$

full NLO result: 2-loop virtual part encoded in a grid based on phase space points which are sparse in the high energy region

→ large uncertainties for $\sqrt{s} \gtrsim 800\,\mathrm{GeV}$

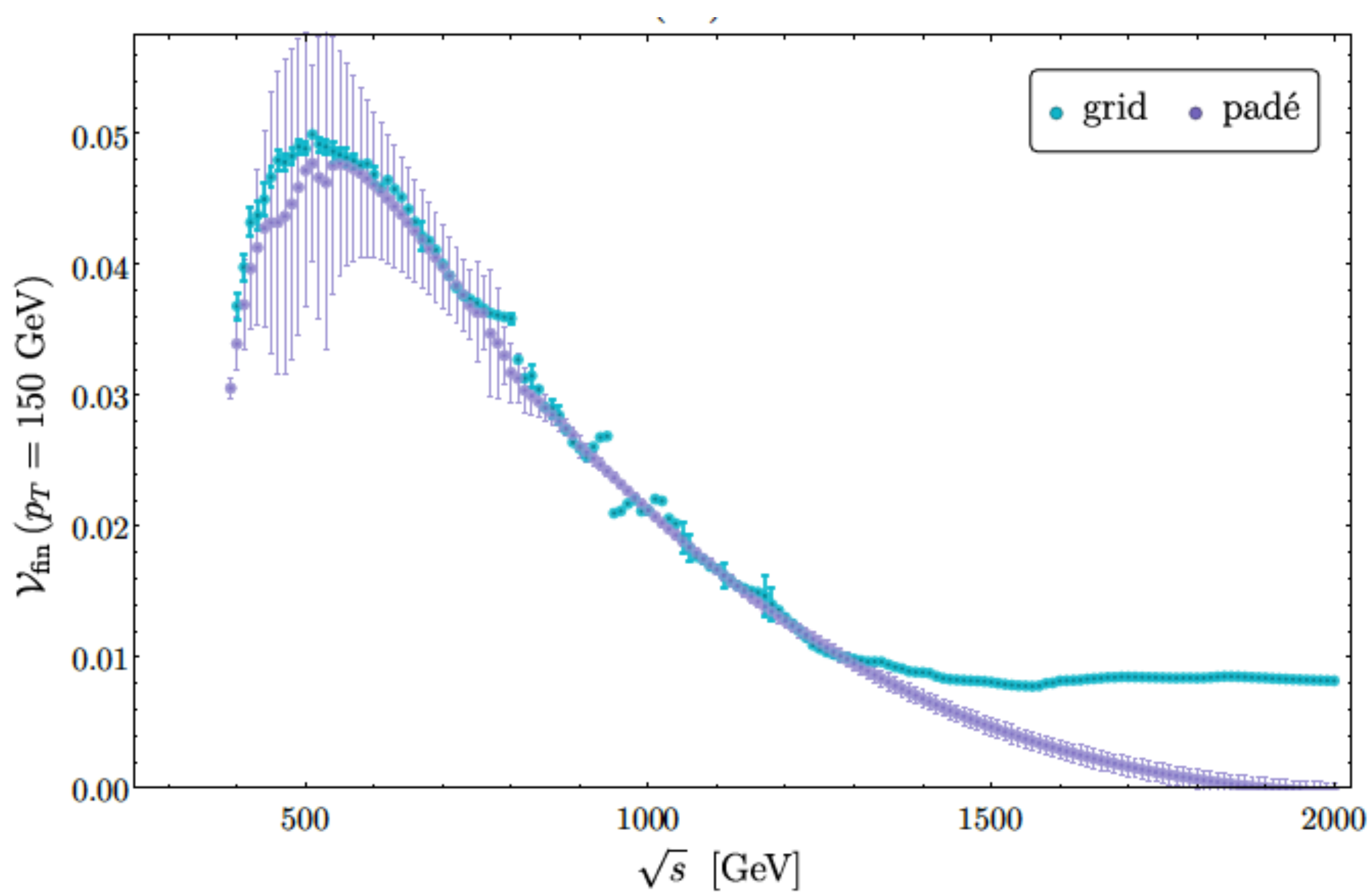

NLO + high energy expansion

high energy expansion: large uncertainties for $\sqrt{s} \lesssim 800\,\mathrm{GeV}$

full NLO result: 2-loop virtual part encoded in a grid based on phase space points which are sparse in the high energy region

→ large uncertainties for $\sqrt{s} \gtrsim 800\,\mathrm{GeV}$

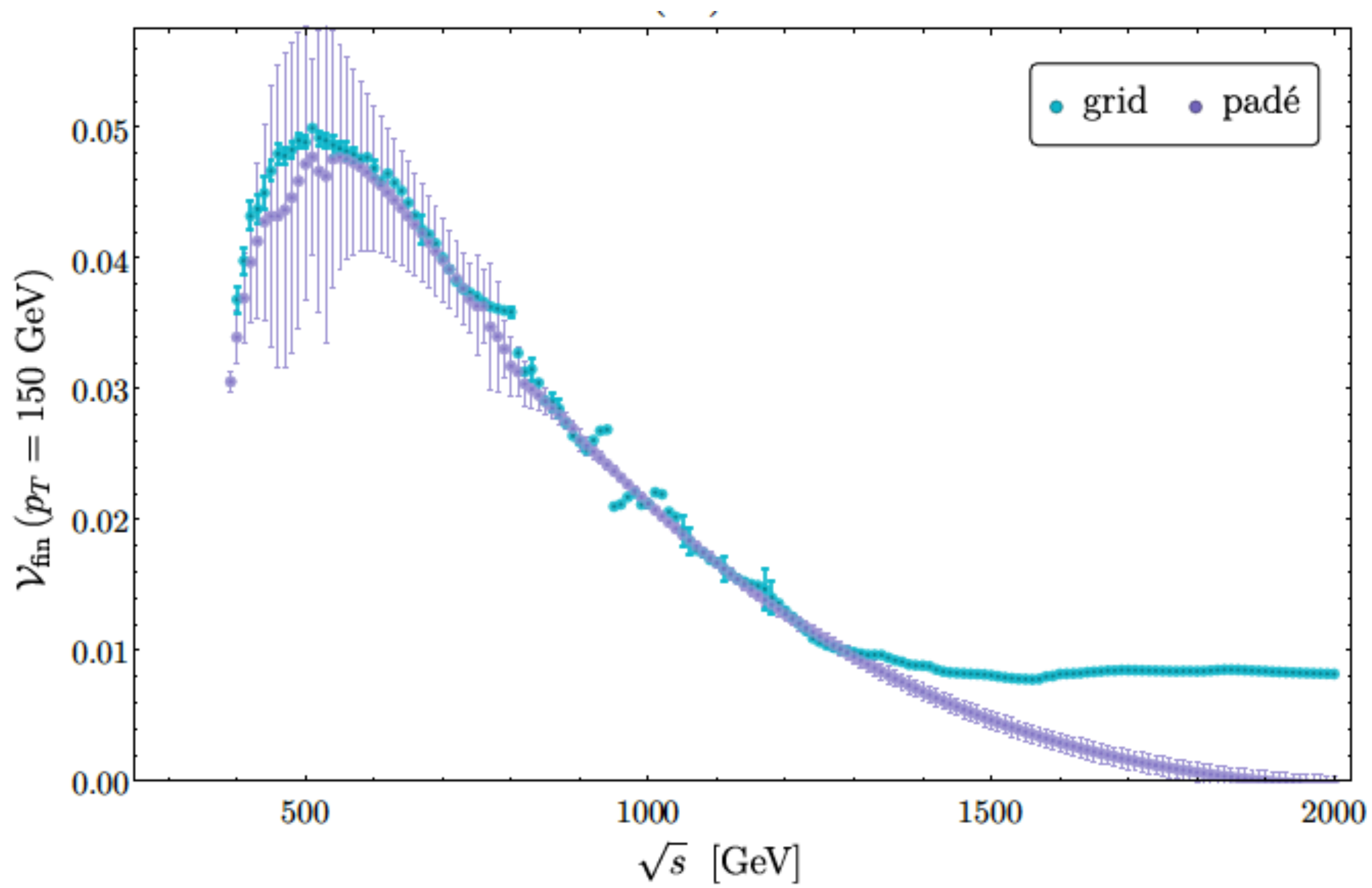

→ combine the two approaches!

Davies, GH, Jones, Kerner, Mishima, Steinhauser, Wellmann ‘19

NLO + high energy expansion

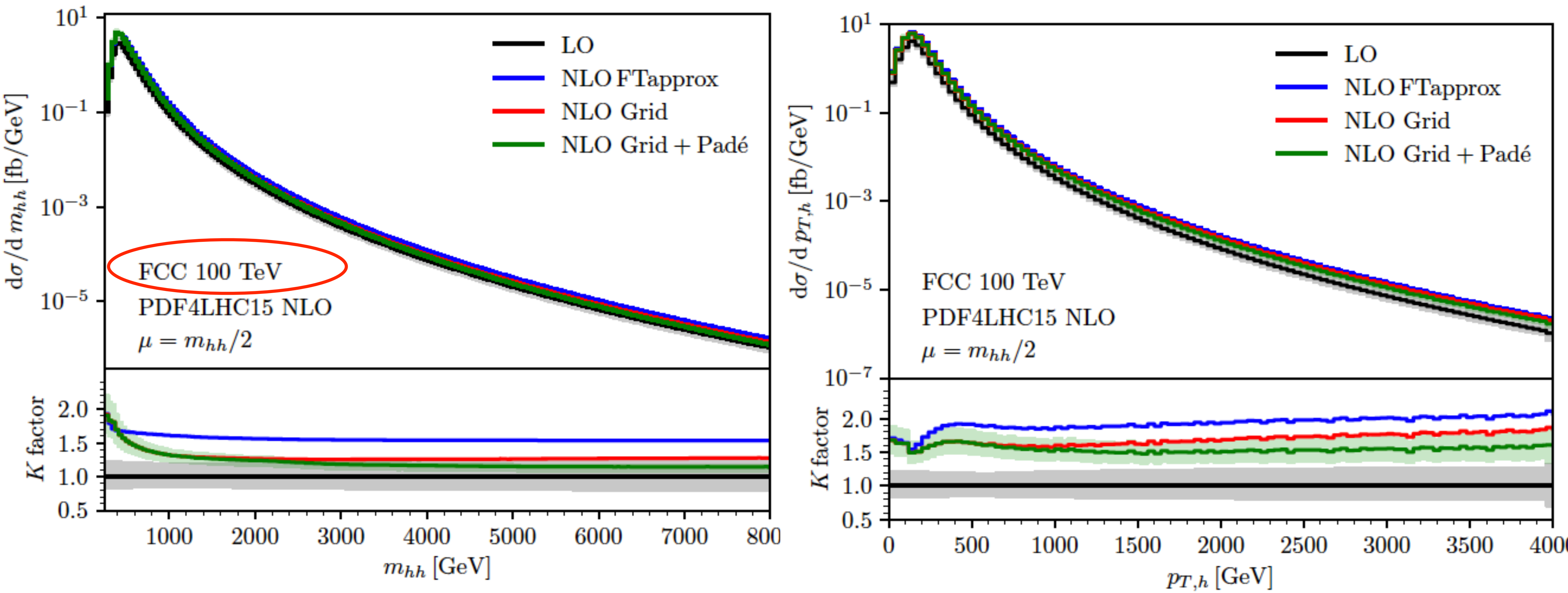

KIT-improved grid https://github.com/mppmu/hhgrid

important at high CMS energies, high invariant mass, pTh

(e.g. boosted Higgs analysis, FCC)

BSM couplings in the Higgs sector

non-linear Effective Field Theory (EFT):

("Electro-Weak Chiral Lagrangian EWChL") [Buchalla et al. '13]

Lagrangian relevant for $gg \to HH$

$$\Delta\mathcal{L}_{d\chi\leq 4} = -m_t \left(c_t \frac{h}{v} + c_{tt} \frac{h^2}{v^2} \right) \bar{t}\, t - c_{hhh} \frac{m_h^2}{2v} h^3 + \frac{\alpha_s}{8\pi} \left(c_{ggh} \frac{h}{v} + c_{gghh} \frac{h^2}{v^2} \right) G^a_{\mu\nu} G^{a,\mu\nu}$$

5 anomalous couplings (SM: $c_{tt} = 0, c_{ggh} = c_{gghh} = 0$)

LO diagrams:

$d\chi \leq 4$

and $\mathcal{O}(g_s^2)$

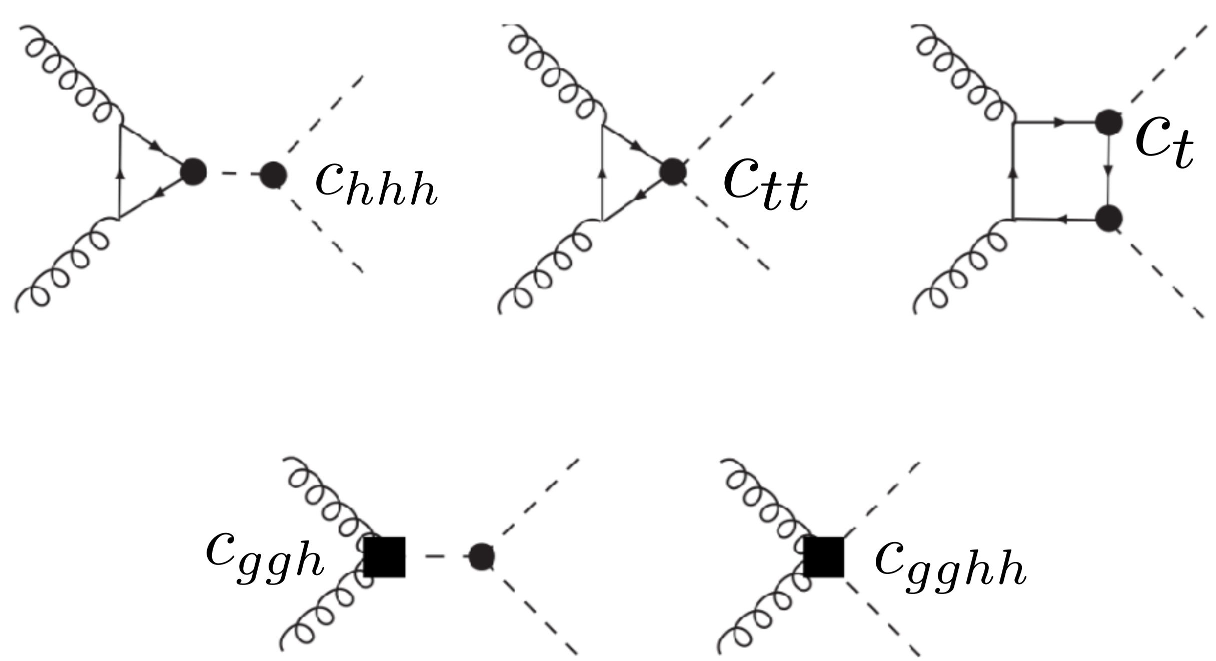

NLO QCD corrections

Buchalla, Capozi, Celis, GH, Scyboz '18

Example diagrams

virtual corrections:

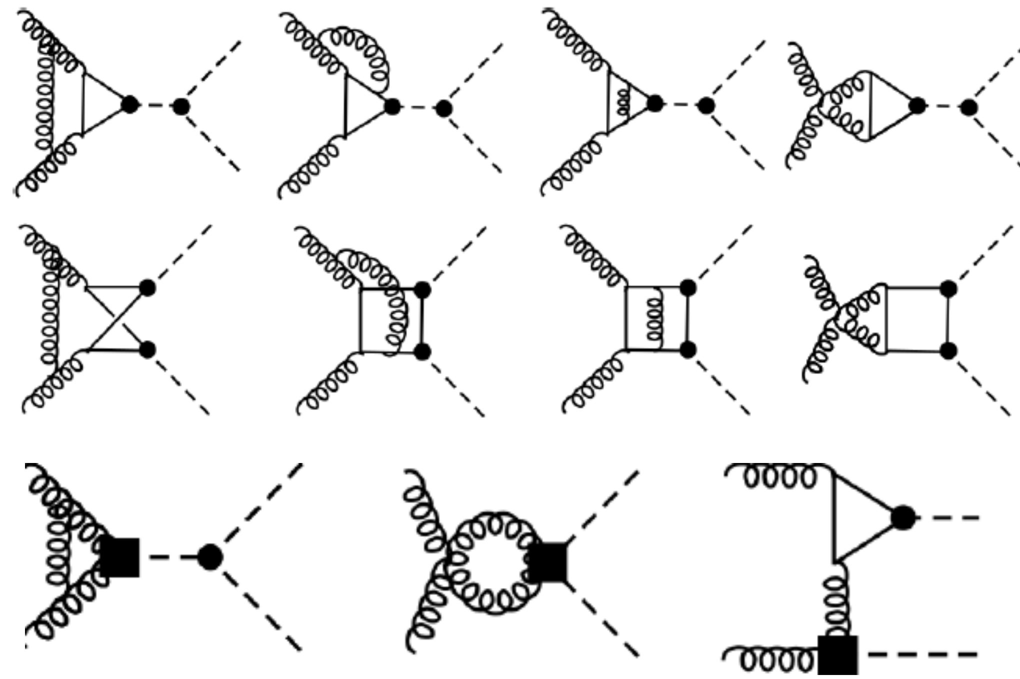

2-loop SM-like

1-loop EFT

real corrections:

5-point 1-loop diagrams

tree diagrams $\propto c_{ggh},\ c_{gghh}$

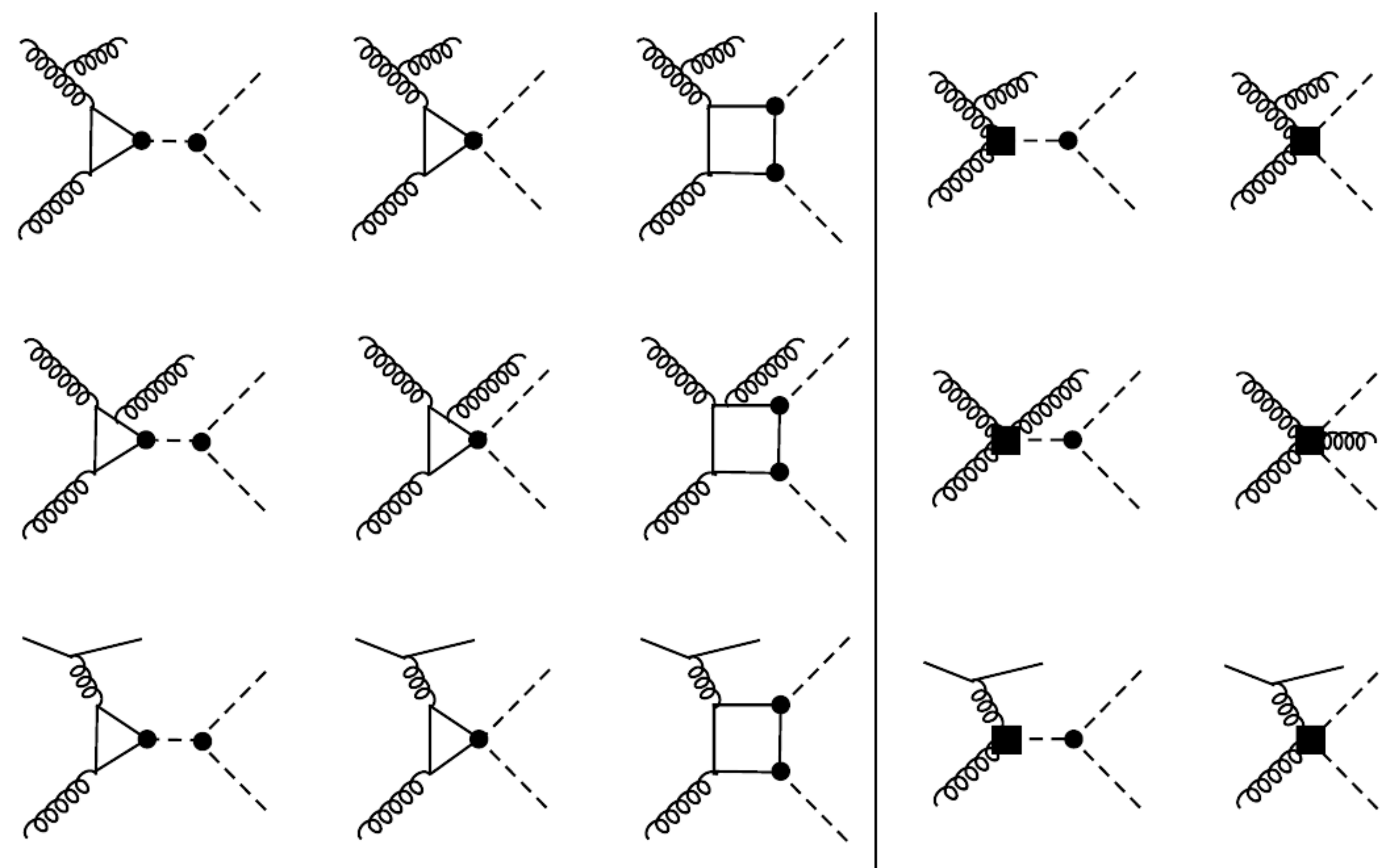

Comparison with approximation $m_t \to \infty$

relative size of corrections as functions of the BSM couplings

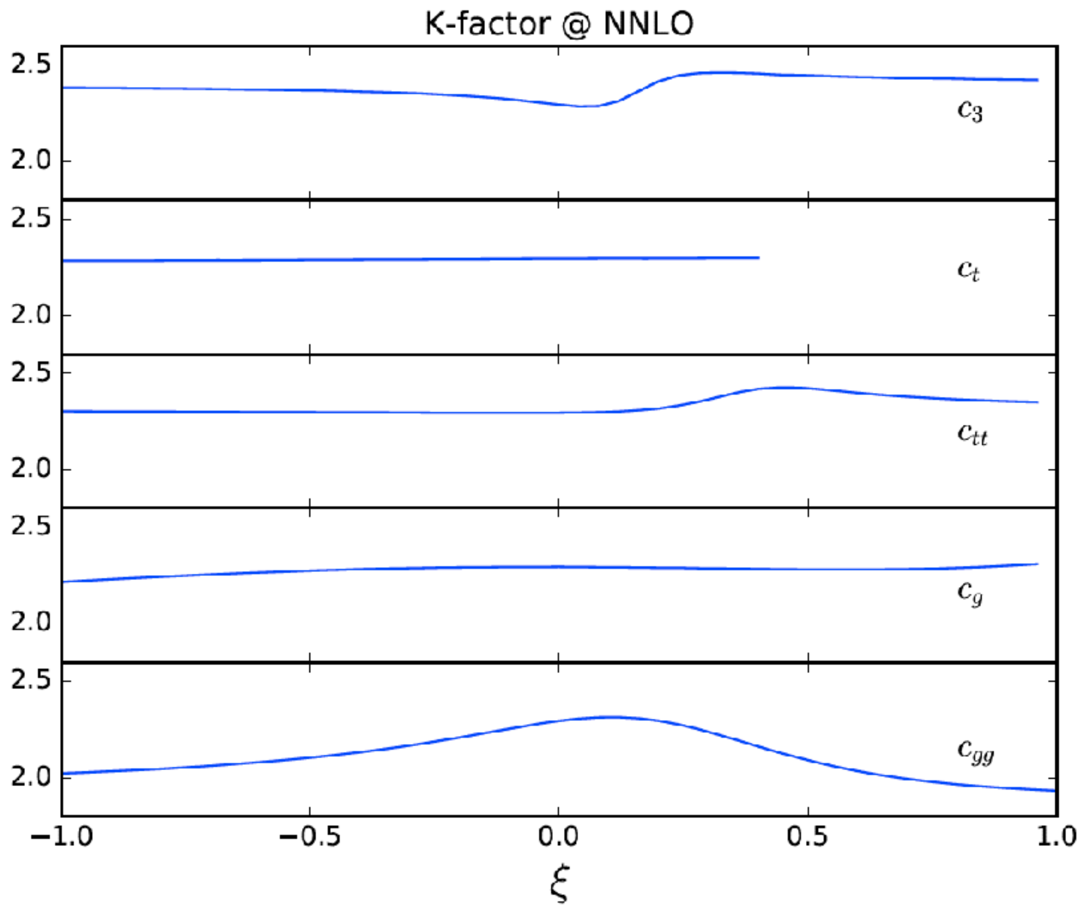

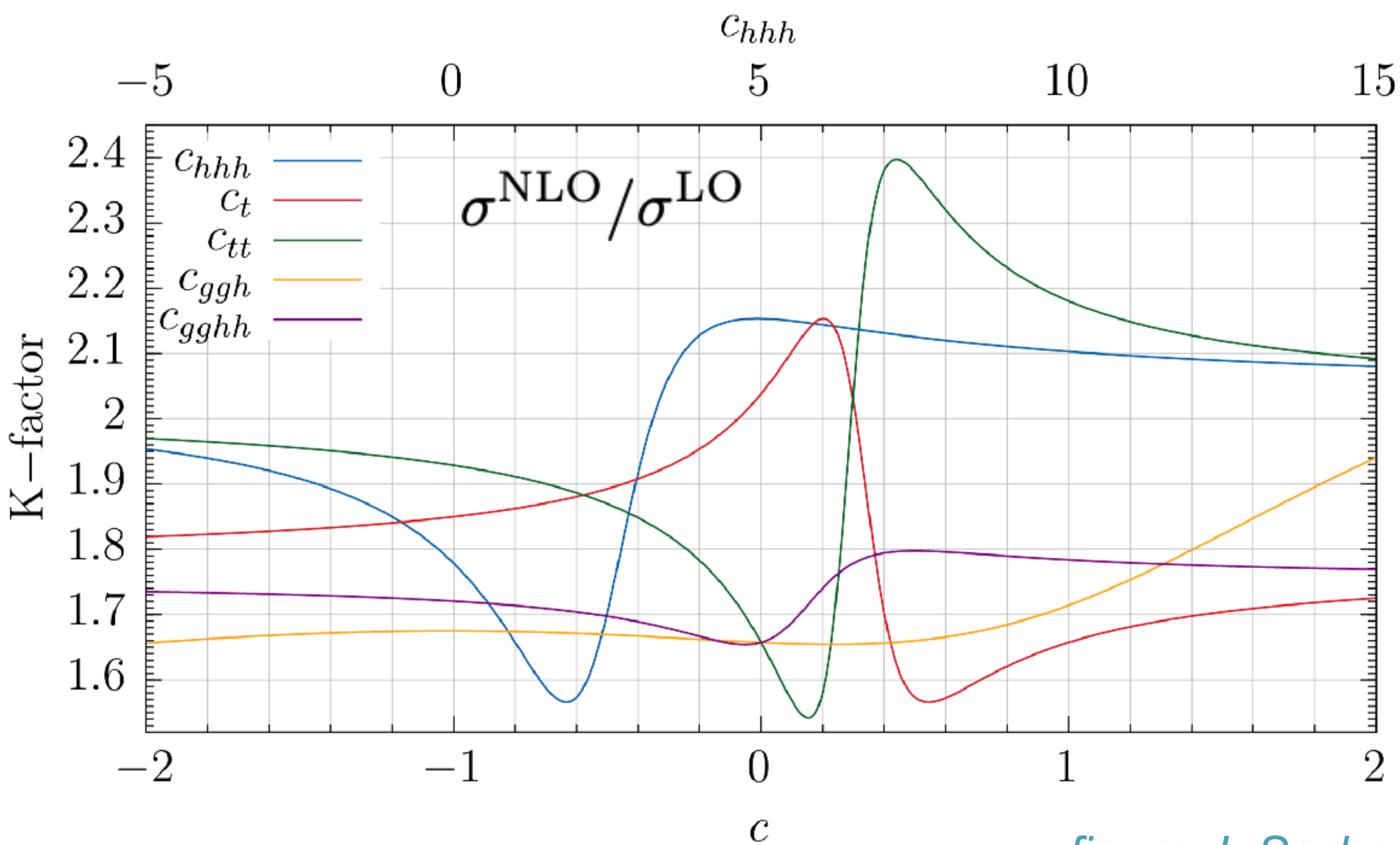

figure: L.Scyboz

NNLO rescaled HTL $(m_t \to \infty)$

De Florian, Fabre, Mazzitelli '17

SM values: $\xi = 0$, $c_3 = 1 + 10\,\xi$

see also

Gröber, Mühlleitner, Spira, Streicher '15

NLO $m_t \to \infty$

NLO with full m_t dependence

Buchalla, Capozi, Celis, GH, Scyboz '18, '19

Comparison with approximation $m_t \to \infty$

relative size of corrections as functions of the BSM couplings

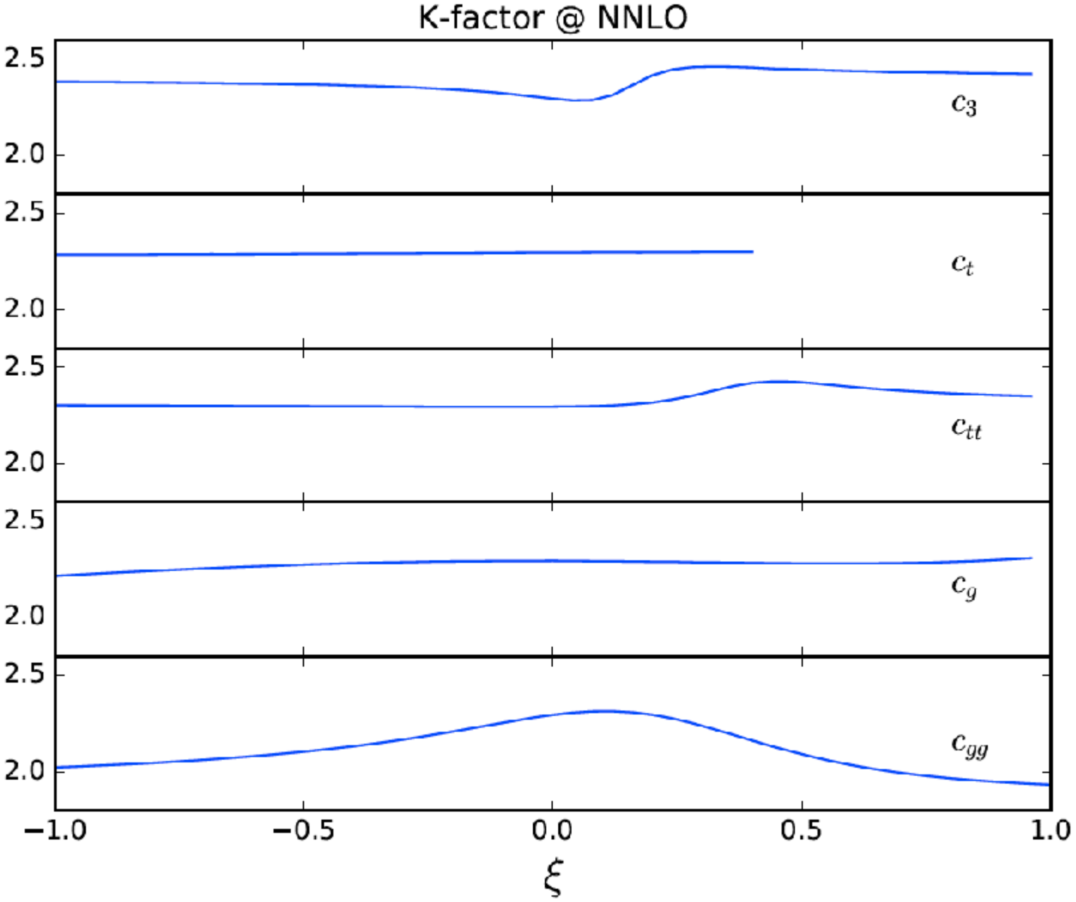

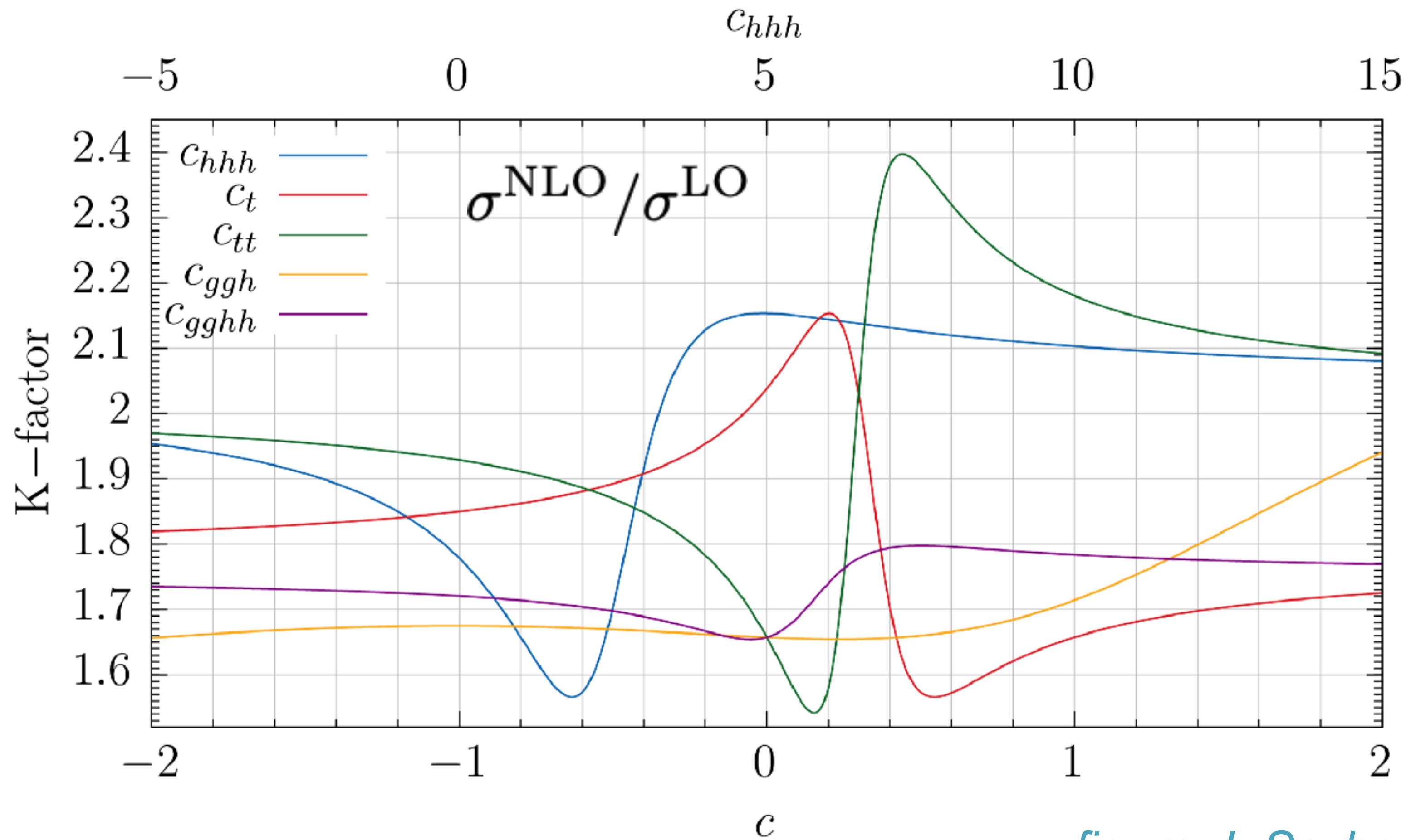

figure: L.Scyboz

NNLO rescaled HTL $(m_t \to \infty)$

De Florian, Fabre, Mazzitelli '17

SM values: $\xi = 0\,,\ c_3 = 1 + 10\,\xi$

see also

Gröber, Mühlleitner, Spira, Streicher '15

NLO $m_t \to \infty$

NLO with full m_t dependence

Buchalla, Capozi, Celis, GH, Scyboz '18, '19

top mass effects on K-factors important!

HH@NLO + Parton Shower

- combinations:

GoSam+Powheg + Pythia 8

MG5_aMC@NLO + Pythia 8

GH, Jones, Kerner, Luisoni, Vryonidou ‘17

Sherpa Jones, Kuttimalai ‘17

GoSam + Powheg + (Pythia 8.2 or Herwig 7.1) GH, Jones, Kerner, Luisoni, Scyboz

1903.08137

- allows to assess shower uncertainties
  (angular ordered and dipole shower in Herwig)

- possibility to vary the trilinear Higgs coupling and
  top-Higgs Yukawa coupling

http://powhegbox.mib.infn.it/User-Process-V2/ggHH

HH invariant mass with variation of the self-coupling

GH, Jones, Kerner, Luisoni, Scyboz '19

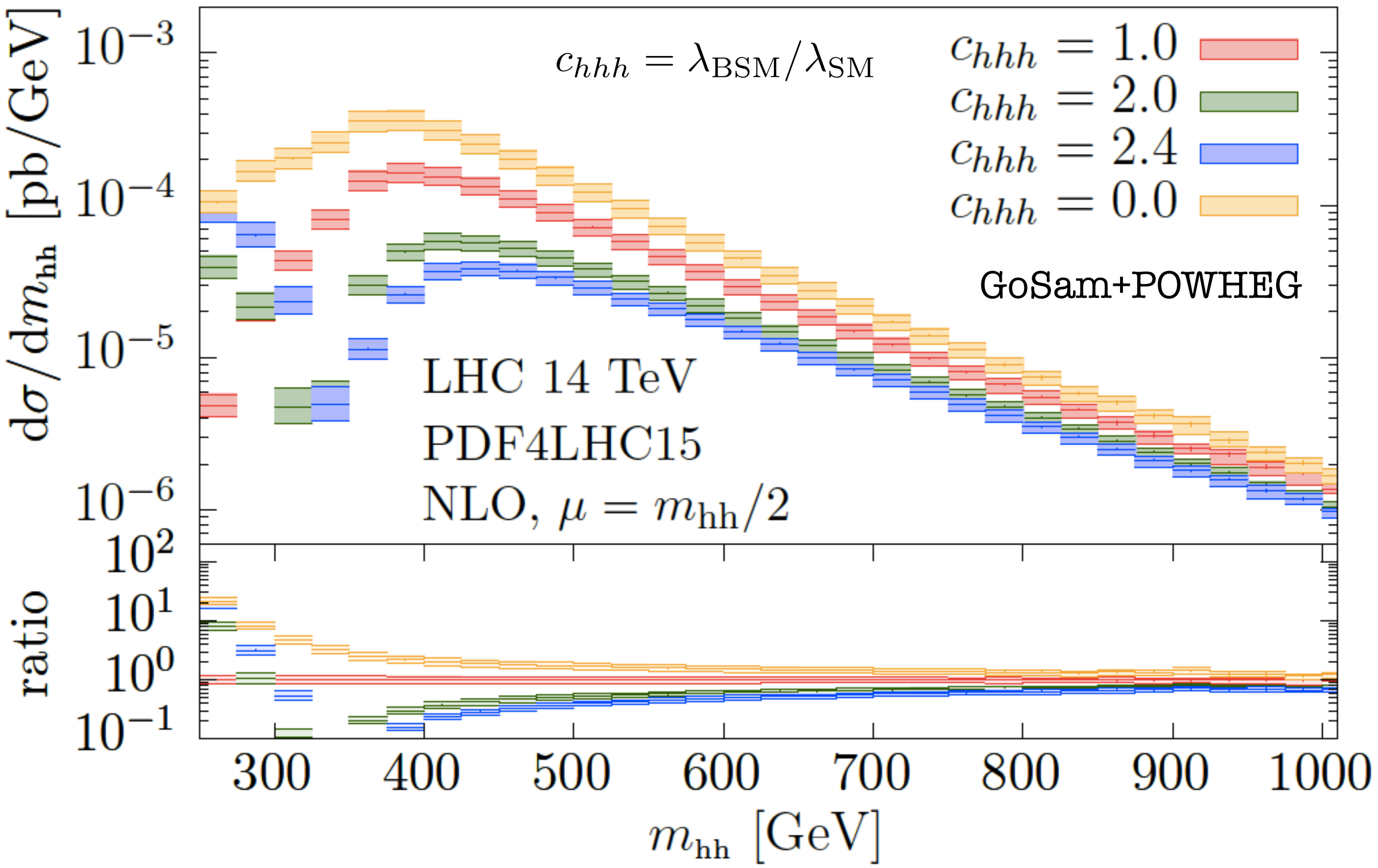

dip in m_{hh} distribution

at 350 GeV for c_{hhh} ~ 2.4

↑

$c_{hhh} = 0$ largest

in this group

bands: 3-point scale variations

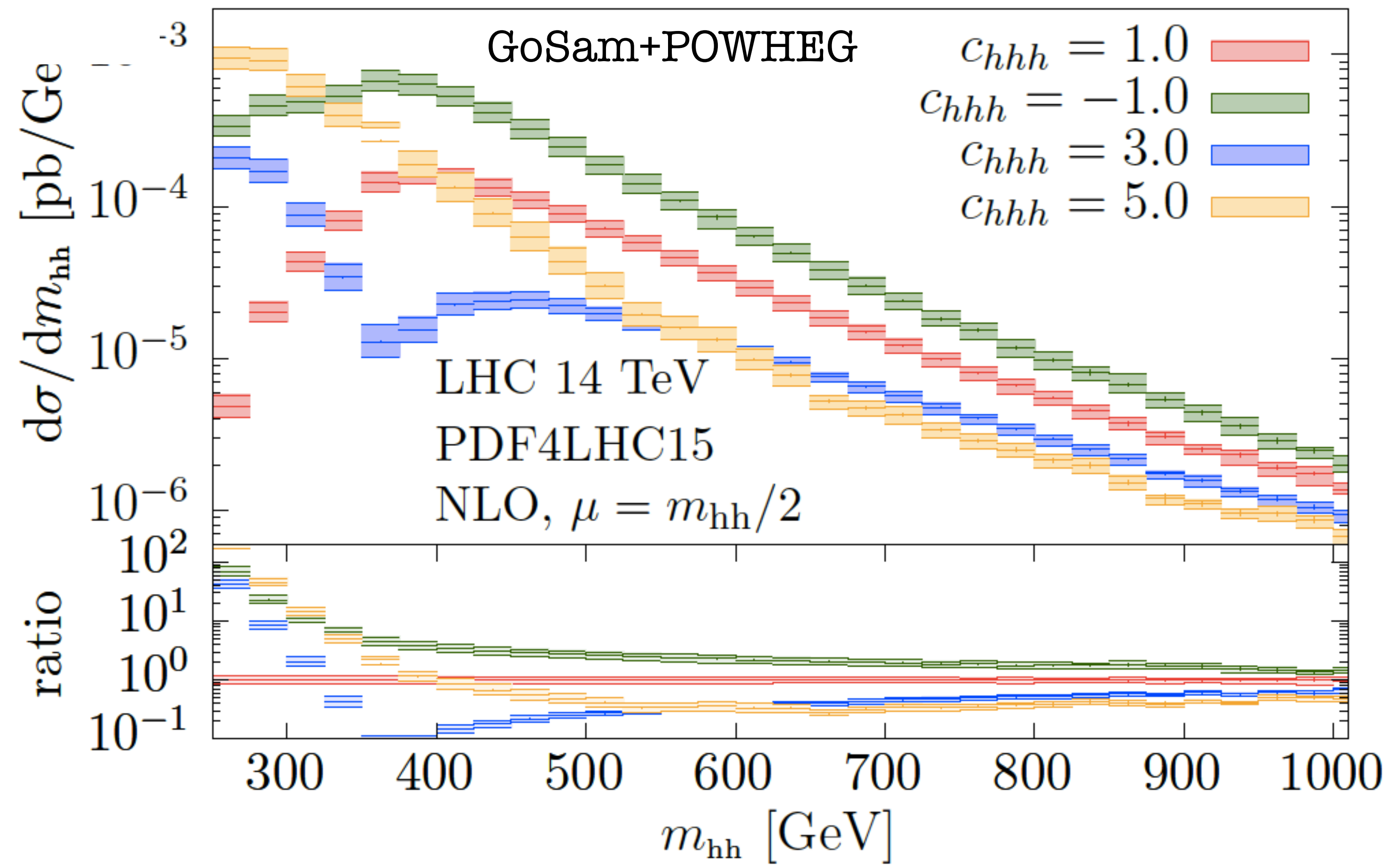

HH@NLO + Parton Shower

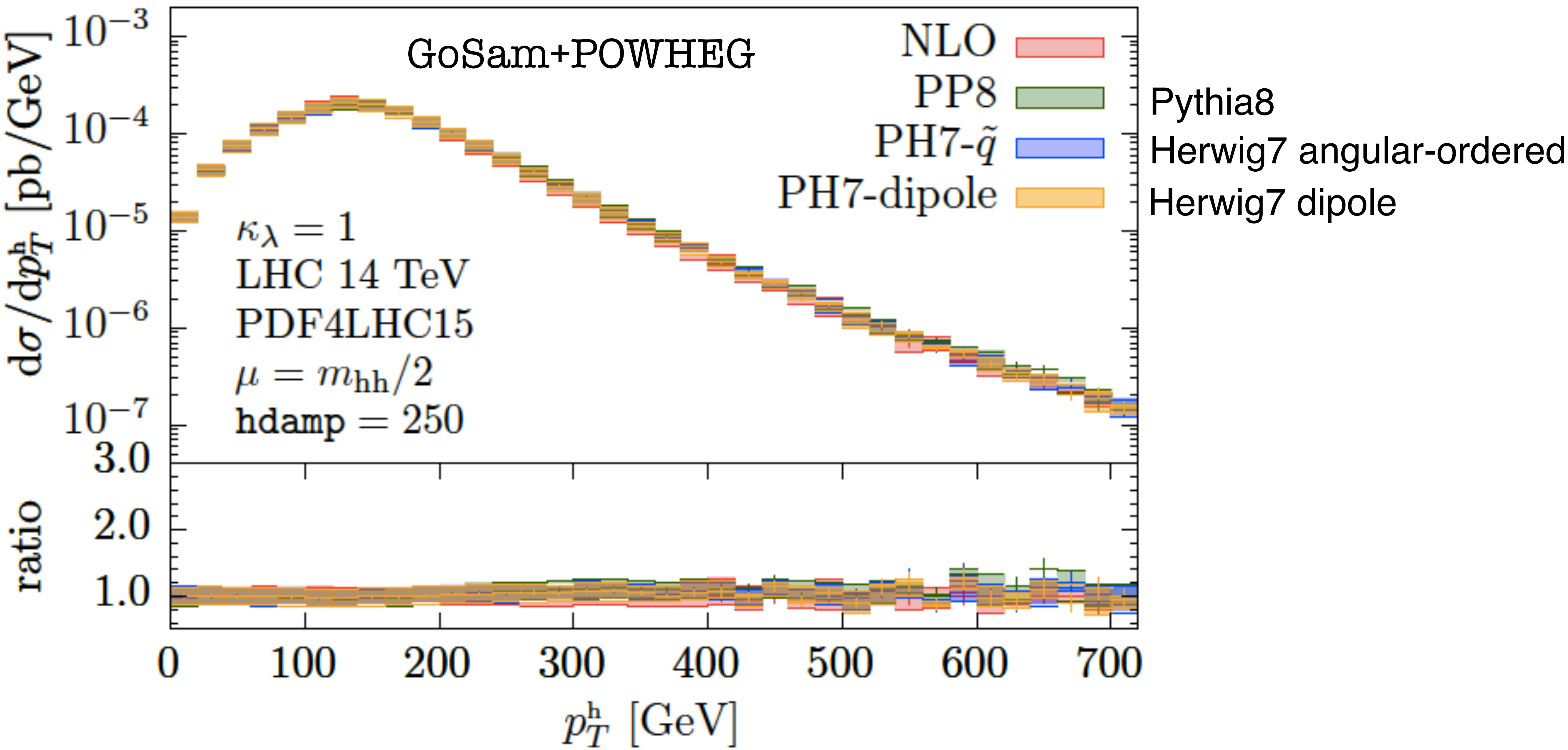

• transverse momentum of one of the Higgs bosons:
inclusive in additional radiation, not very sensitive to shower differences

HH@NLO + Parton Shower

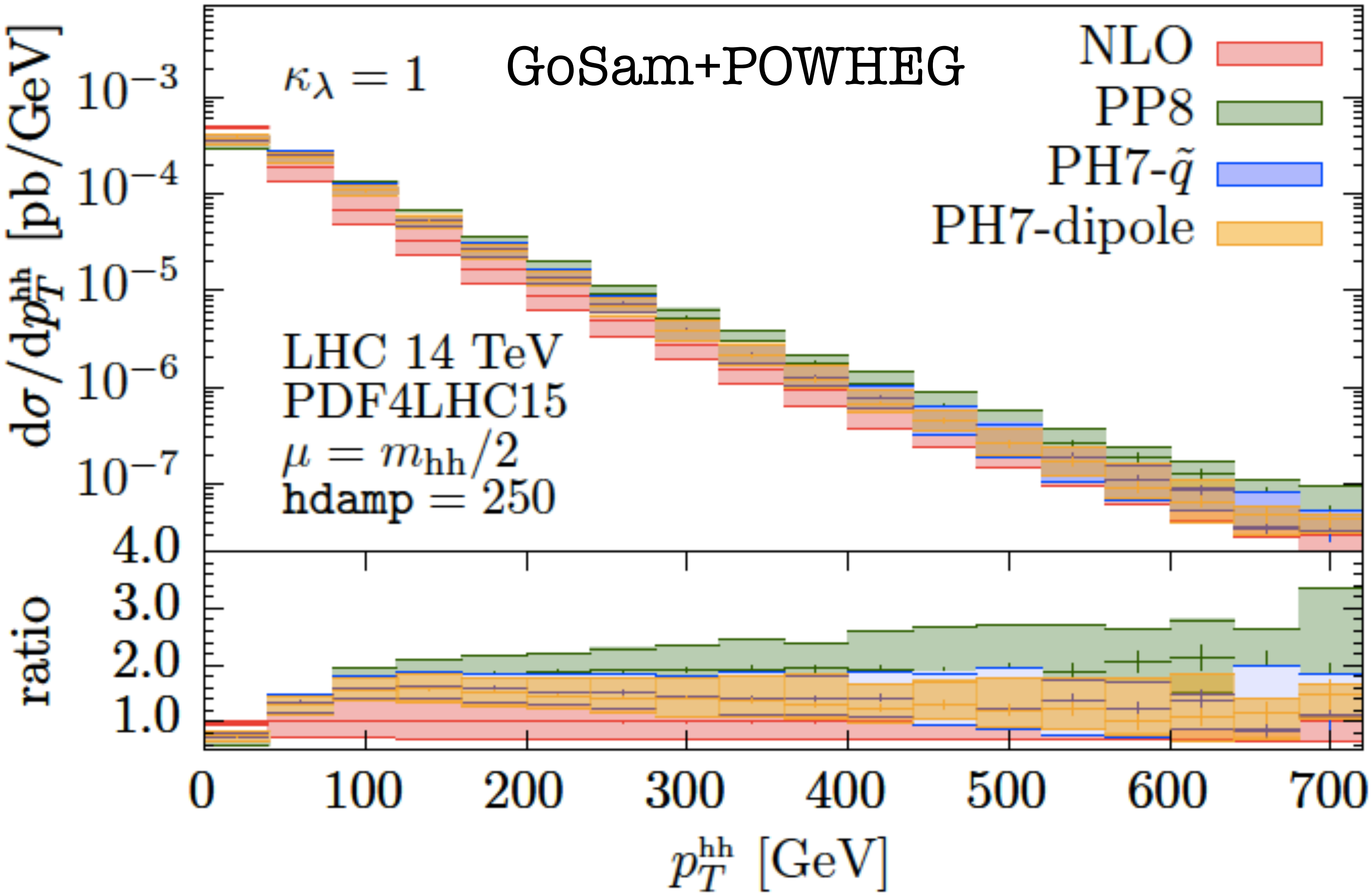

Pythia8

Herwig7 angular-ordered

Herwig7 dipole

$$p_T^{hh} = \vec{p}_T^{\,h_1} + \vec{p}_T^{\,h_2}$$

transverse momentum of Higgs boson pair: NLO is first non-trivial order

→ very sensitive to extra radiation

Pythia8 produces relatively hard additional jets (also seen in other processes, e.g. ZZ, WW, H)

m_{hh} shape analysis

We have found that values of c_{hhh} around 2.4 lead to a dip/double peak structure in the m_{hh} distribution

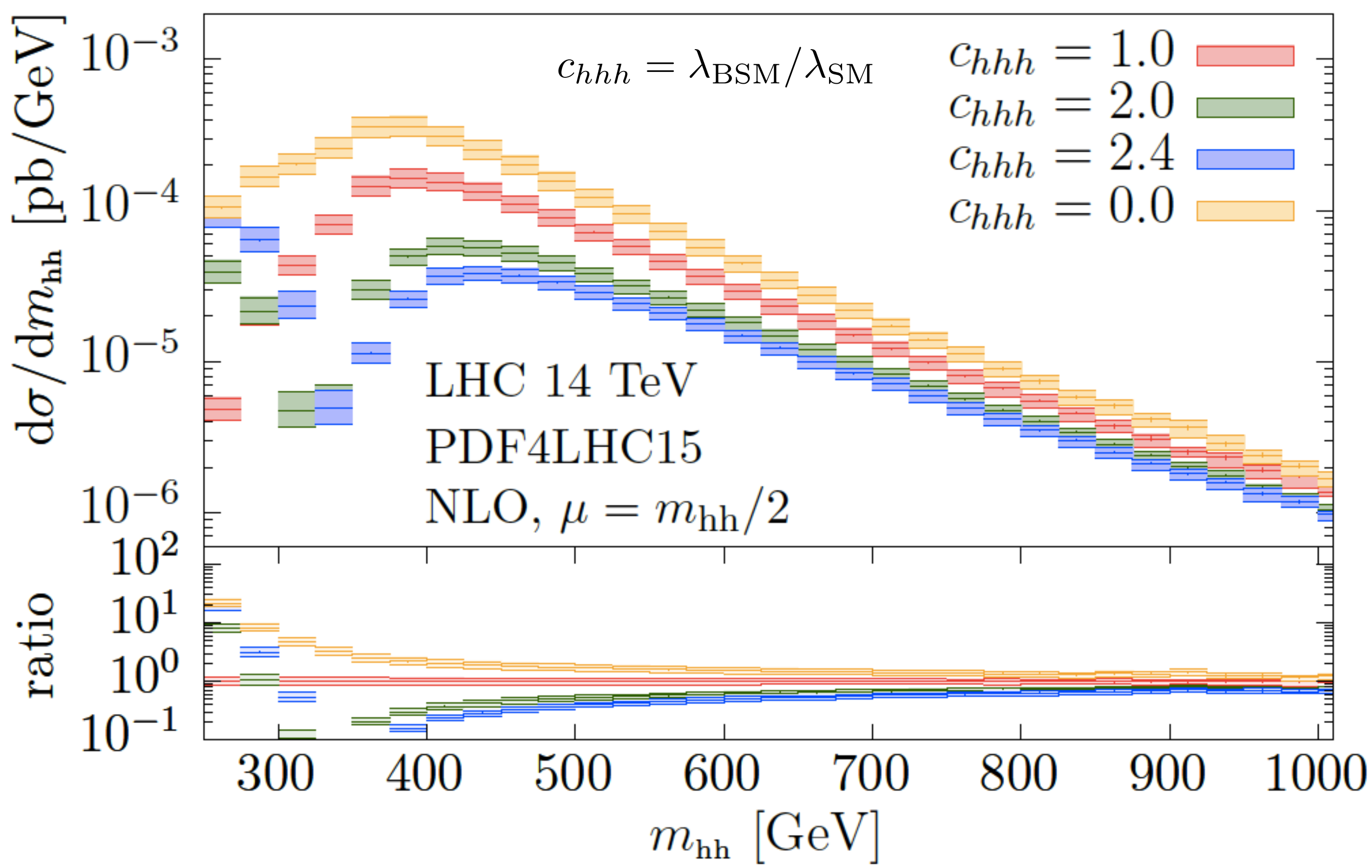

Is this feature preserved once variations of the other couplings are taken into account?

HH pair invariant mass distribution

$$c_{hhh} = 2.4, c_t = 1, c_{tt} = 0, c_{ggh} = 2/3, c_{gghh} = 1/3$$

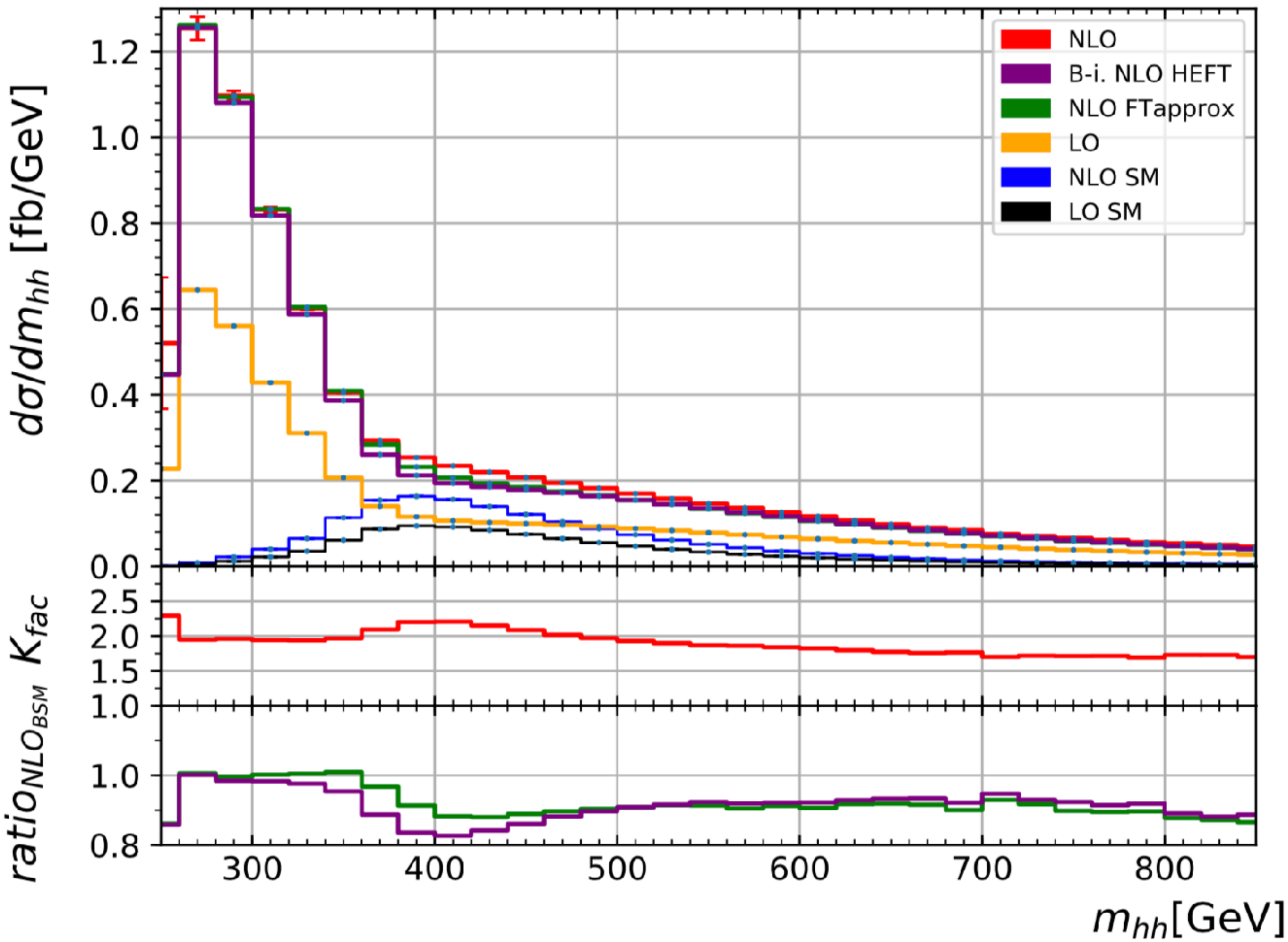

dip destroyed by $c_{ggh}, c_{gghh} \neq 0$

HH pair invariant mass distribution

$$c_{hhh} = 1, c_t = 1, c_{tt} = 0.5, c_{ggh} = 4/15, c_{gghh} = 0.$$

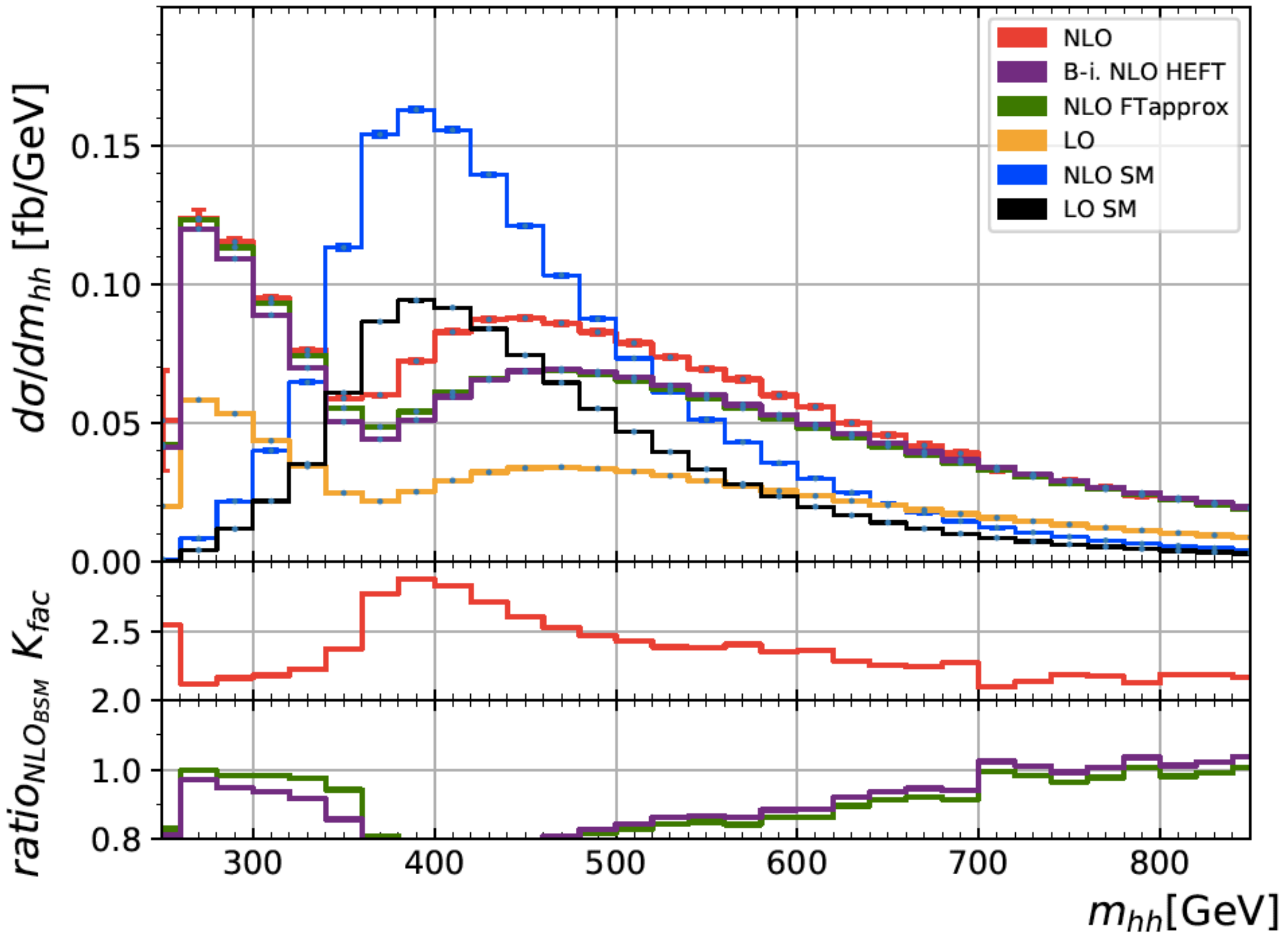

dip, even though $c_{hhh} = 1, c_t = 1$

m_{hh} shape analysis

Aim:

get a clearer idea how the different anomalous couplings affect the shape of the m_{hh} distribution

How?

- find a suitable “measure” defining a characteristic shape type
- visualise underlying parameter space in 2-dim. projections

studied: (a) bin-by-bin analyser script
(b) machine learning

Shape analysis has been done before, but only at LO

see e.g. C.-R. Chen, I. Low ‘14
Azatov, Contino, Panico, Son ‘15
Dawson, Ismail, Low ‘15
Carvalho, Dall’Osso, Dorigo, Goertz, Gottardo, Tosi ’15, ’16
Carvalho, Goertz, Mimasu, Gouzevitch, Aggarwal ‘17

Shape analysis

- use unsupervised learning to identify shape types

- autoencoder from KERAS (tensorflow)

  encoder will try to find common patterns in order to achieve a compressed representation of the data

- input: m_{hh} distributions with 30 bins of width 20 GeV

- produce grid of 10^5 coupling combinations, retain 10% for validation

- then use KMeans algorithm (scikit-learn) for clustering into given number of clusters

```
input_data = Input(shape=(30,))
encoded = Dense(20, activation='relu')(input_data)
encoded = Dense(20, activation='relu')(encoded)
encoded = Dense(4, activation='relu')(encoded)
decoded = Dense(20, activation='relu')(encoded)
decoded = Dense(20, activation='relu')(decoded)
decoded = Dense(30, activation='sigmoid')(decoded)
autoencoder = Model(input_data, decoded)
```

Shape analysis

asking the `KMeans` algorithm for 4 clusters:

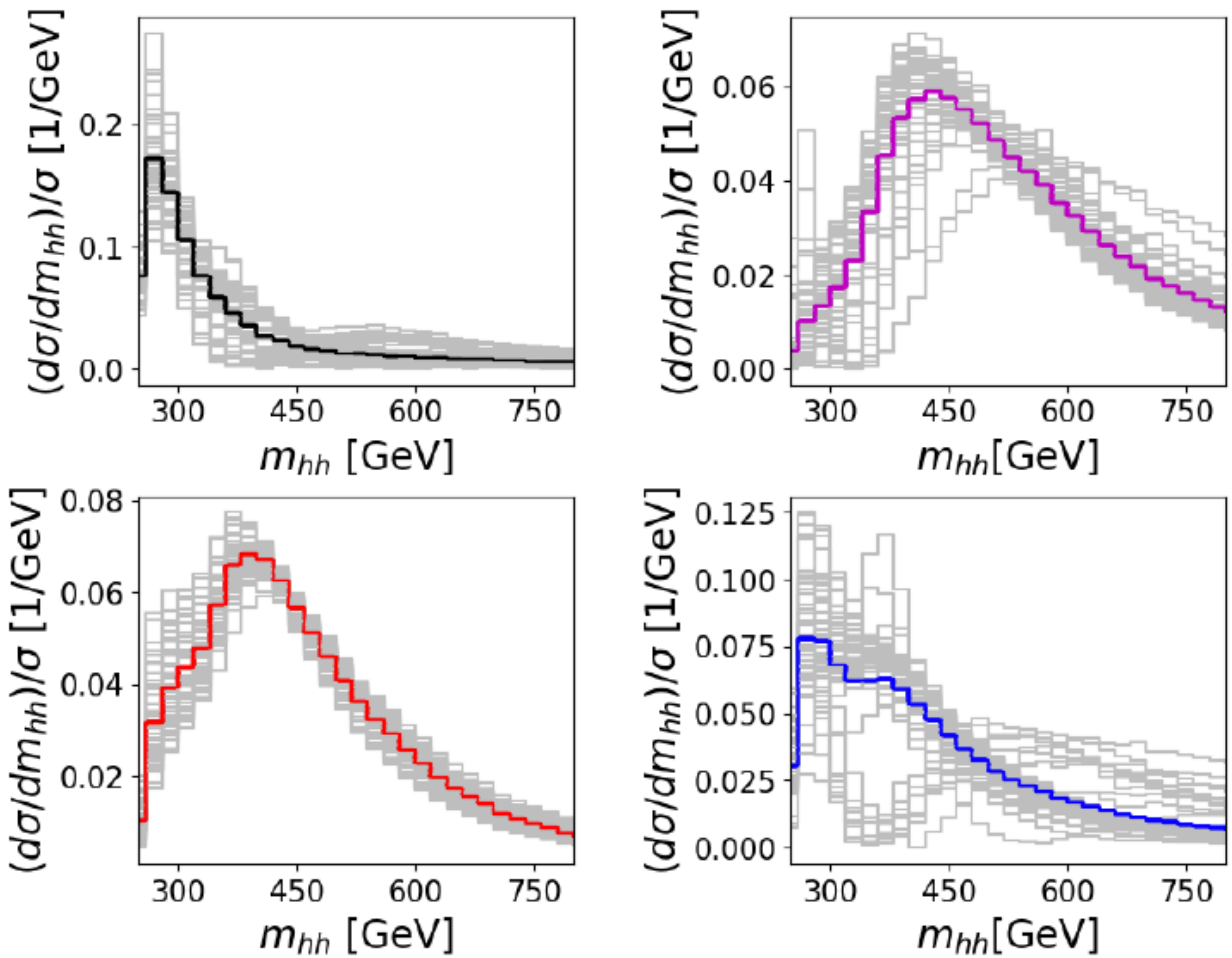

coloured:
cluster centres

too unspecific $\Rightarrow$

ask for more clusters

Shape analysis

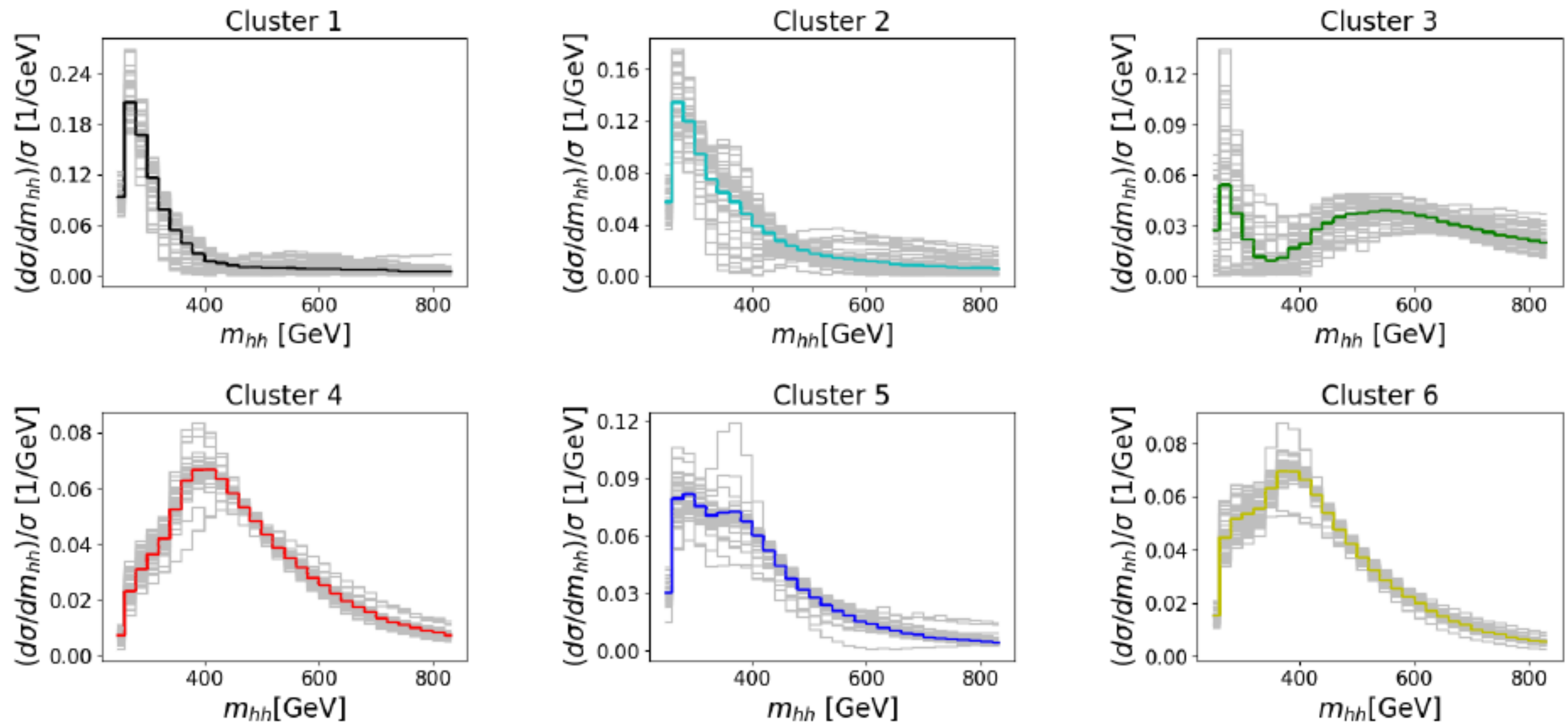

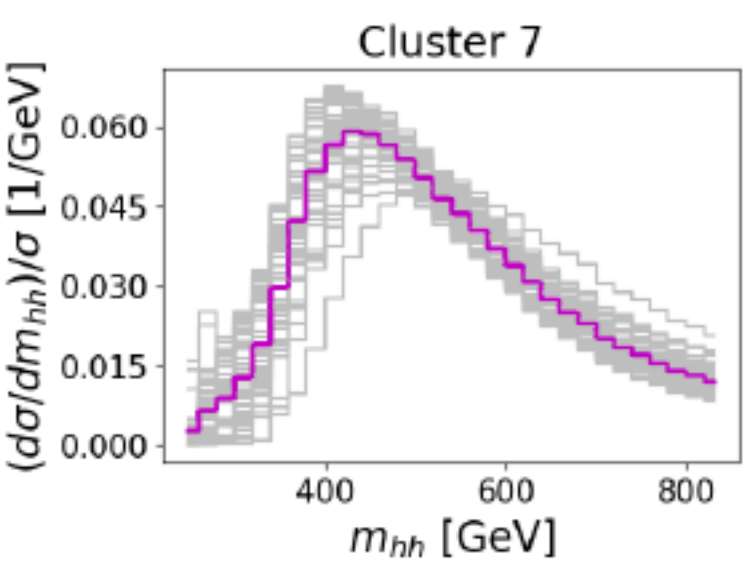

tried 4-8 clusters, 7 seemed to be optimal

Shape analysis: results

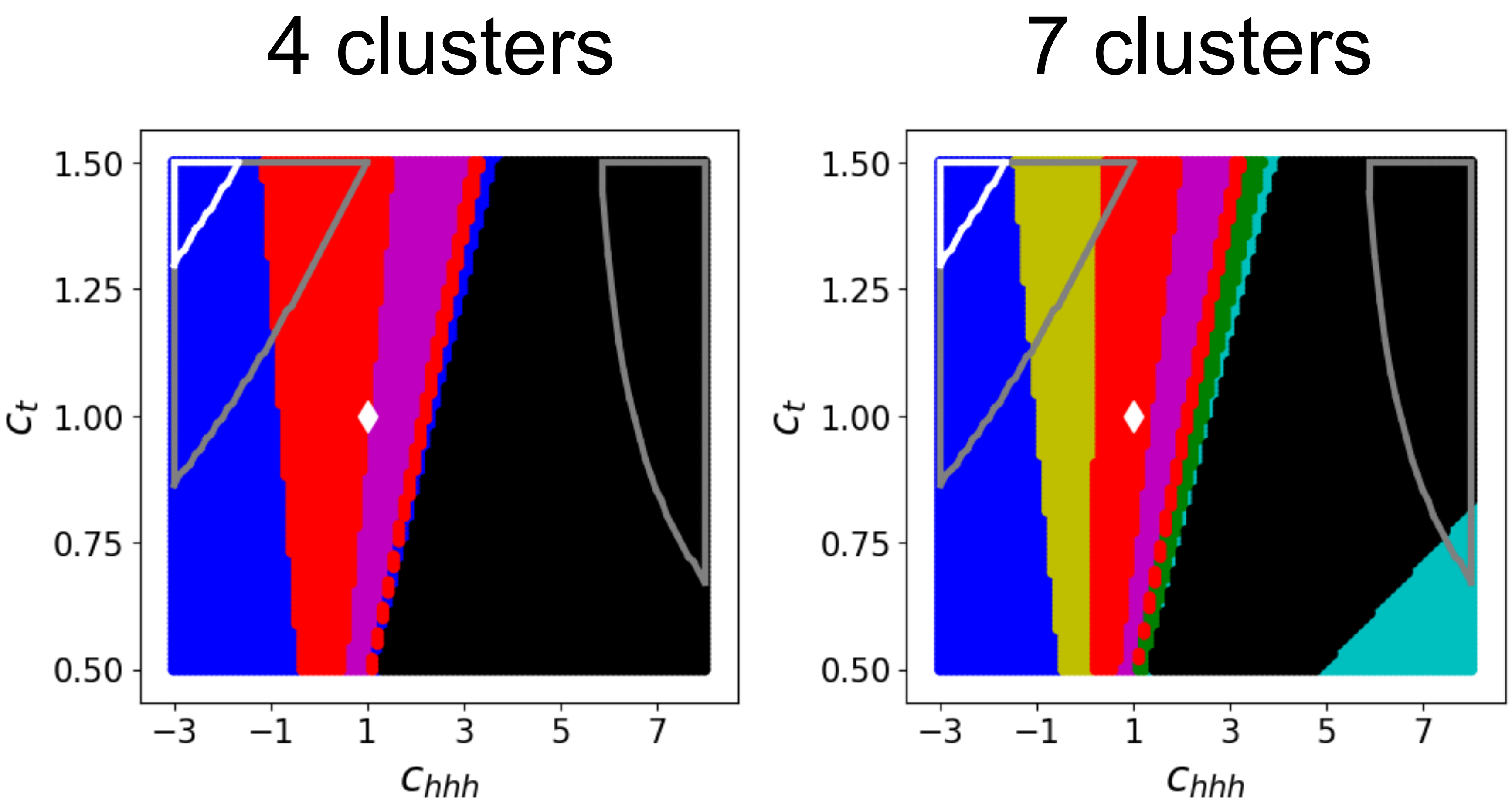

red: SM-like, magenta: enhanced tail, **black**: enhanced low m_{hh}

silver lines: limits on total cross section $\sigma^{HH}_{\mathrm{max}} = 6.9 \times \sigma_{SM}$ (ATLAS)

white lines: CMS limits

- influence of c_{hhh} on the shape much stronger than the one of c_t
- unsupervised clustering able to distinguish small deviations from SM-like shape

Shape analysis

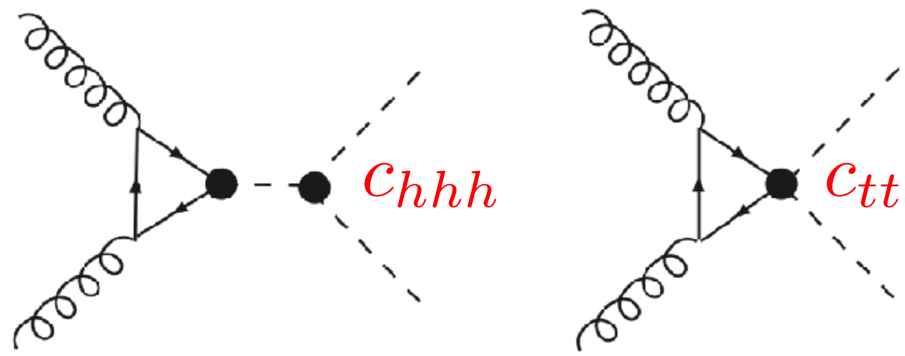

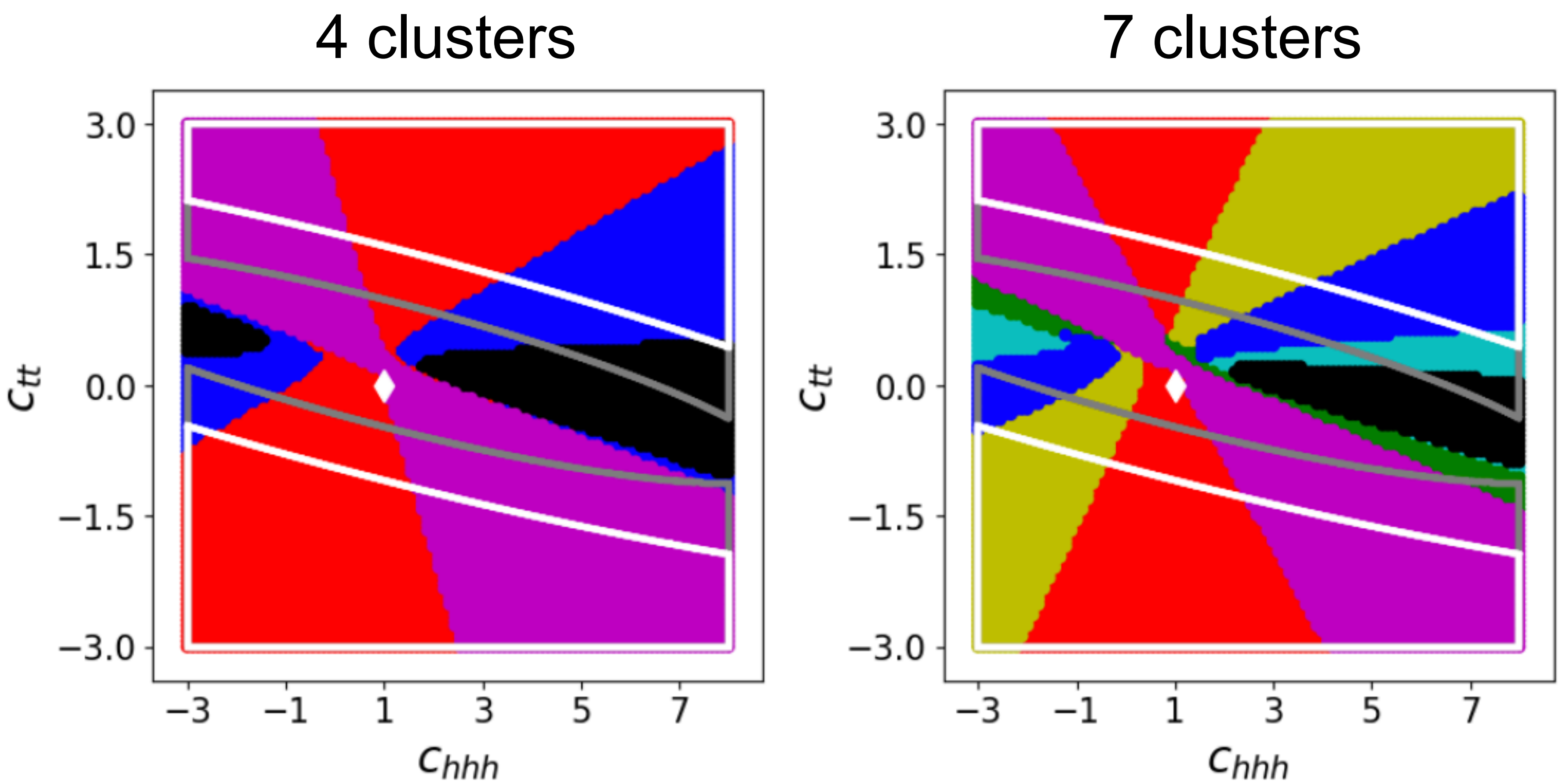

c_{tt} also has strong influence on shape

- region where SM shape is produced is rather small
- shape combined with bounds on total cross section puts constraints on c_{tt}

Summary & Outlook

- NNLO_approx contains top quark mass dependence as far as available, scale dependence reduced to ~5%
- Improved predictions in tails of distributions by combination of full NLO with high energy expansion
- Implementation of gg to HH at full NLO including variations of trilinear coupling and top-Yukawa coupling in Powheg
- Machine learning lends itself to do shape analysis
- Shape analysis combined with bounds on total cross section can help to constrain EFT parameter space

Summary & Outlook

- NNLO_approx contains top quark mass dependence as far as available, scale dependence reduced to ~5%
- Improved predictions in tails of distributions by combination of full NLO with high energy expansion
- Implementation of gg to HH at full NLO including variations of trilinear coupling and top-Yukawa coupling in Powheg
- Machine learning lends itself to do shape analysis
- Shape analysis combined with bounds on total cross section can help to constrain EFT parameter space

Thank you for your attention

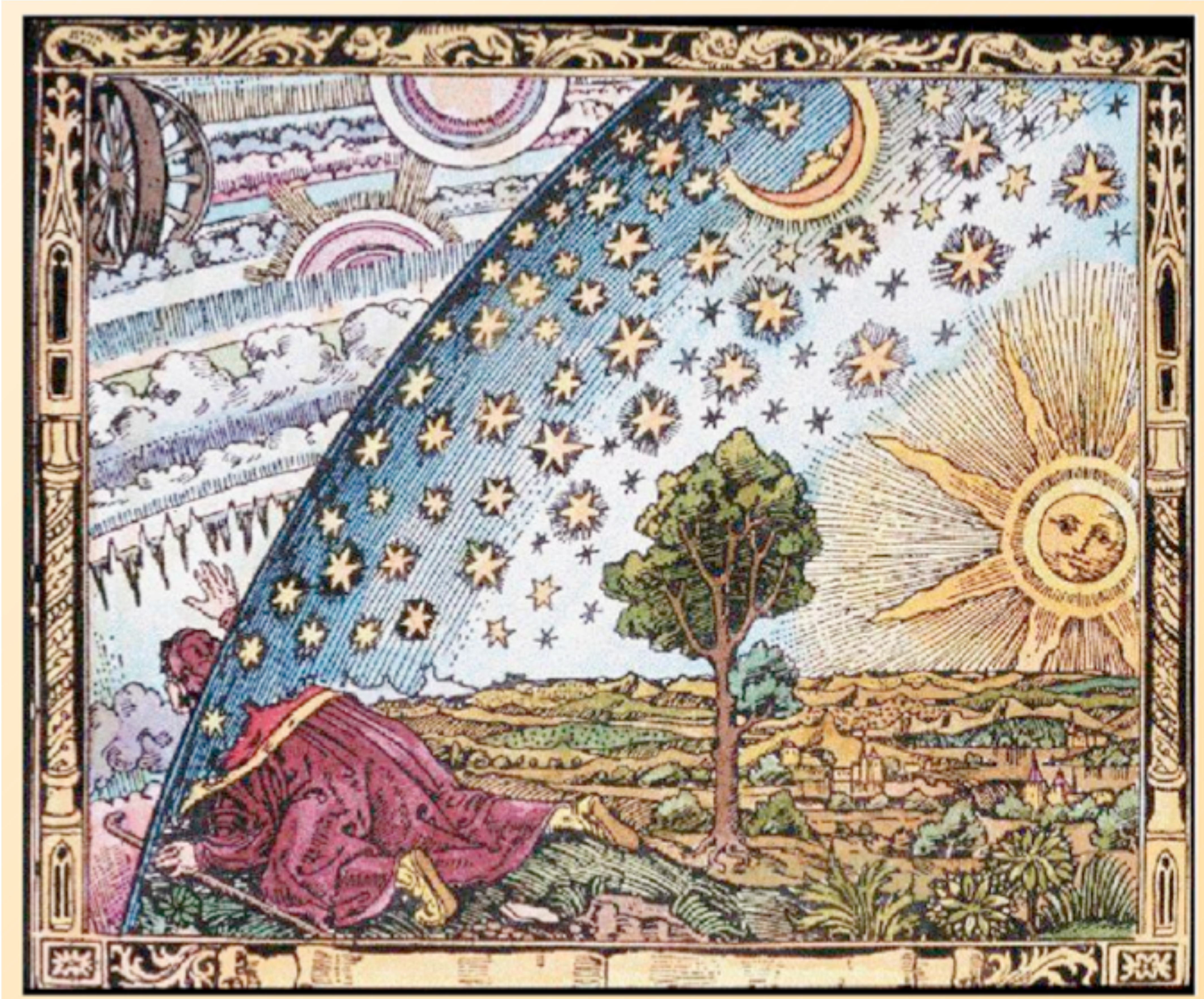

BACKUP SLIDES

Shape analysis

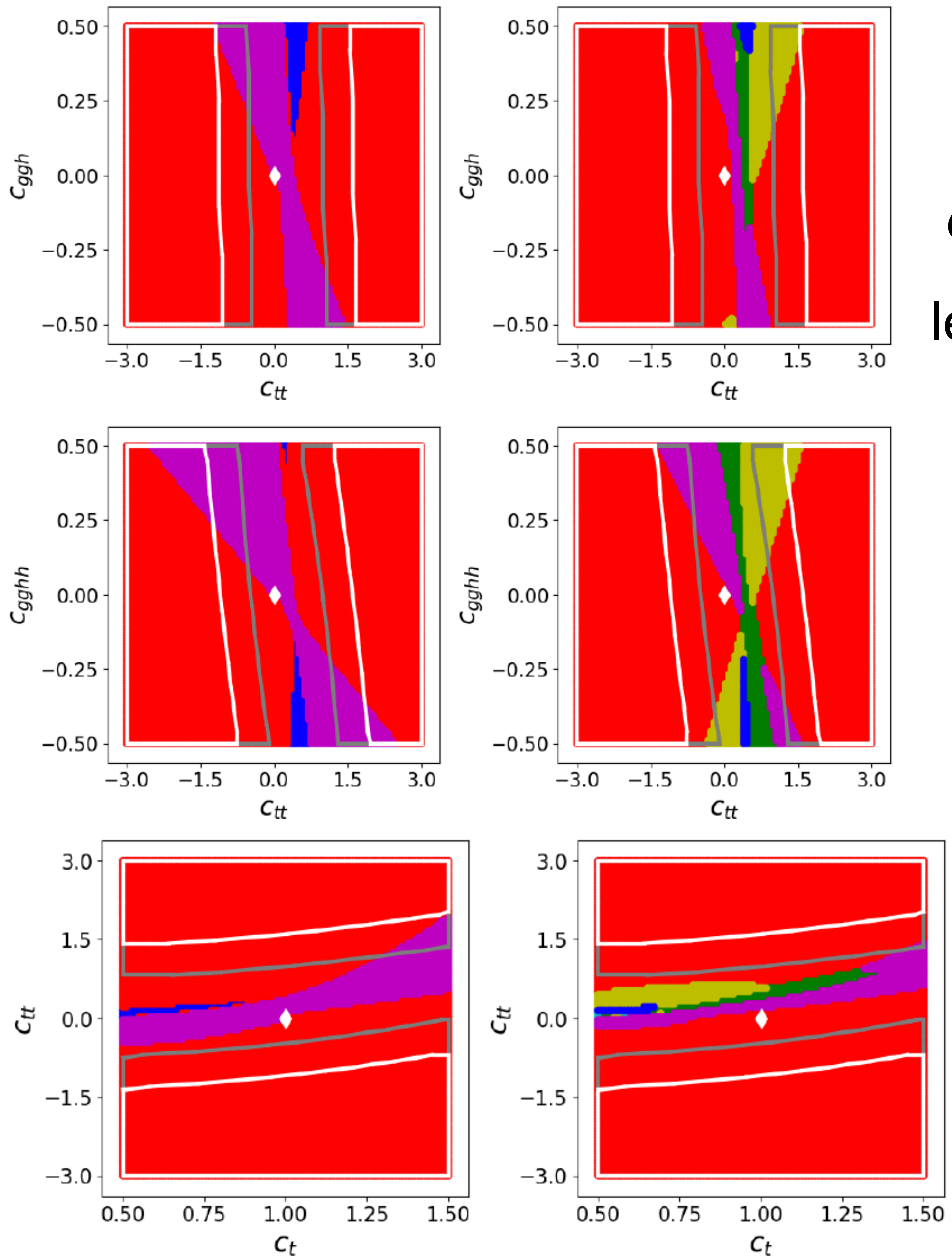

c_{tt} values not too far from zero lead to interesting shape features

Shape analysis: results

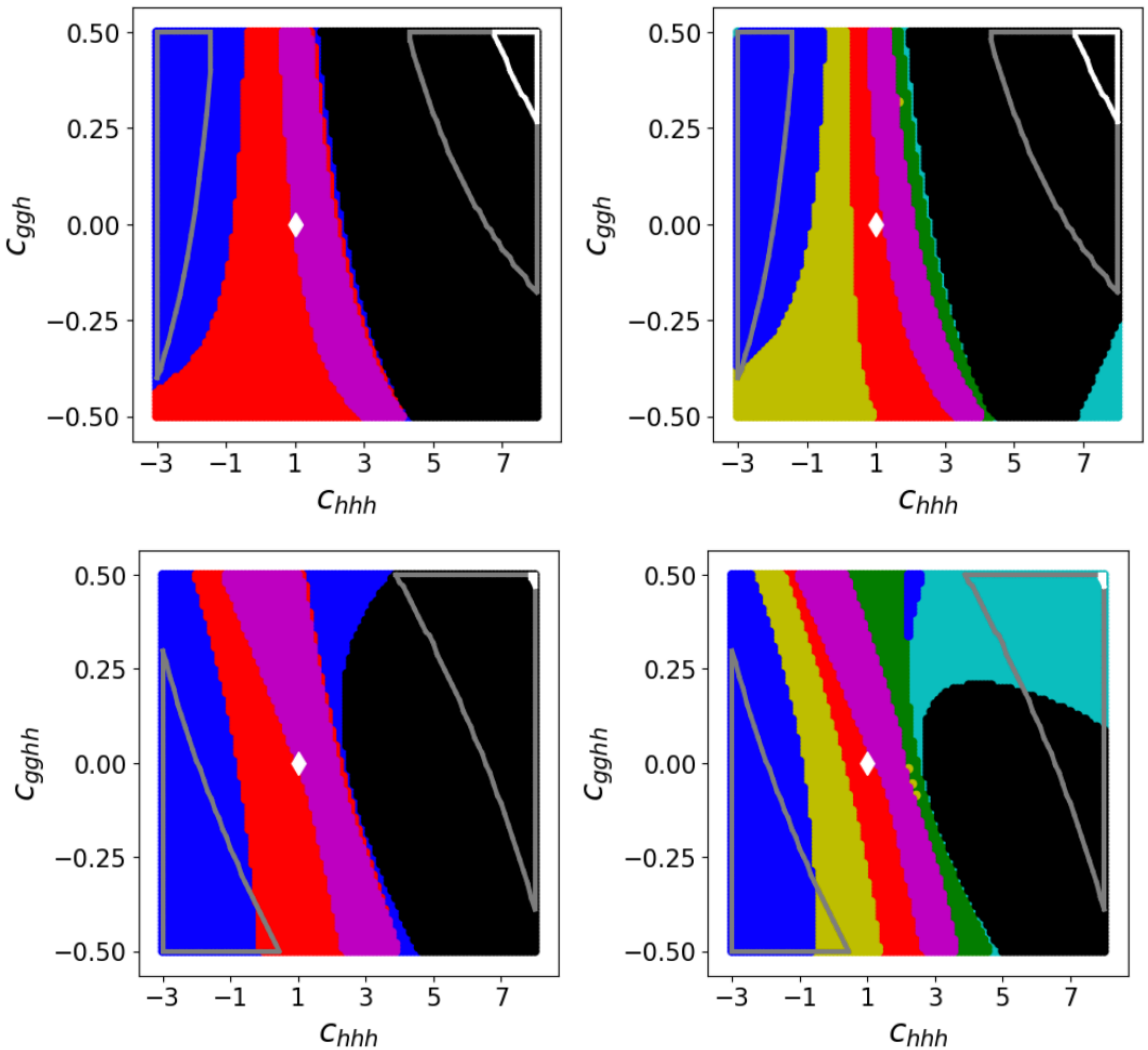

- influence of c_{ggh}, c_{gghh} on the shape also rather mild, tendency to enhance tail and total cross section
- enhanced low m_{hh} region not possible for SM value of c_{hhh}

constraints on ggH and top Yukawa couplings

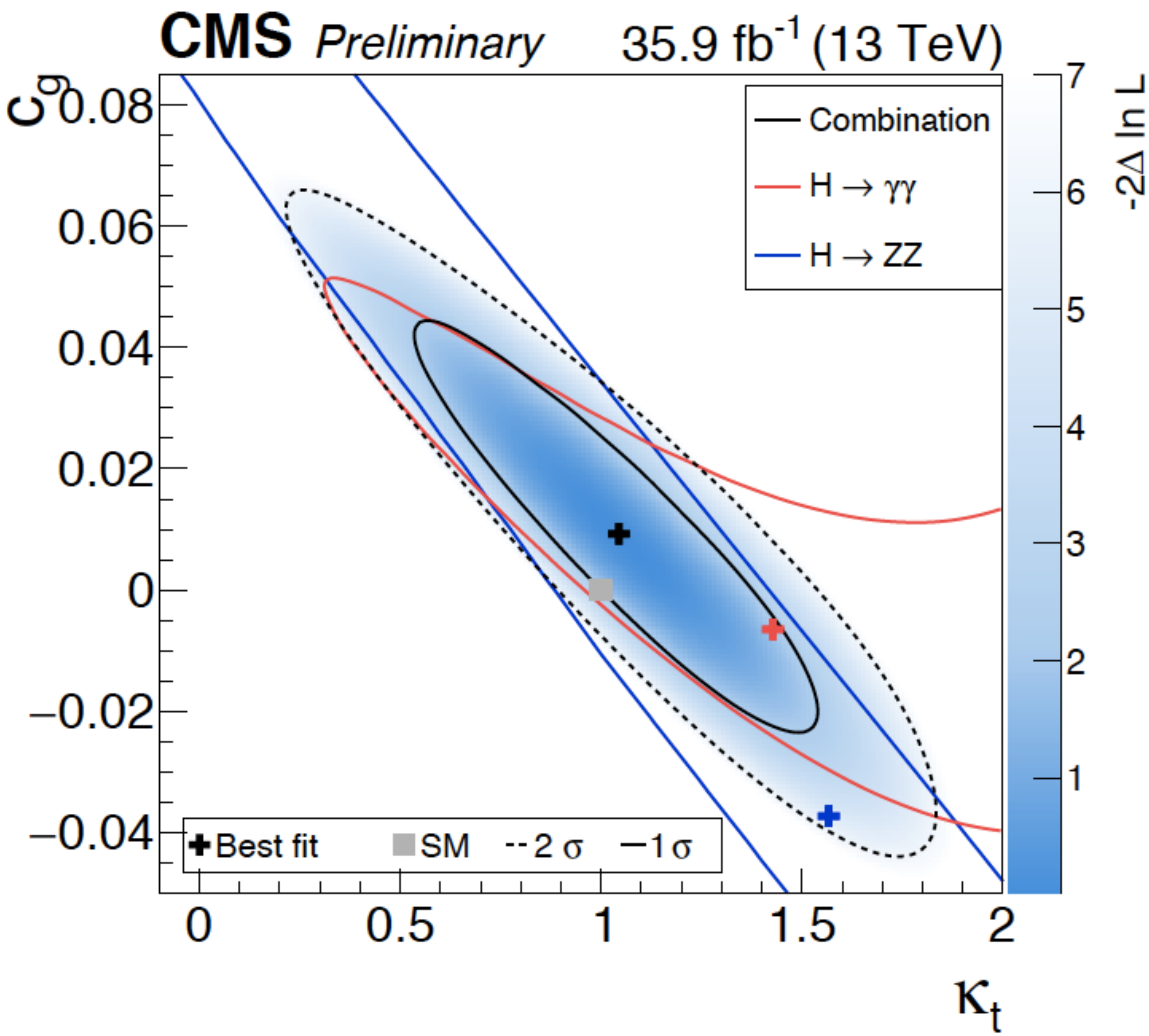

1812.06504

c_{ggh} and c_t
are already quite well constrained from other processes (single Higgs, ttH)

note: $c_{ggh} = 8\, c_g$

Lambda- and mt-dependence of K-factors

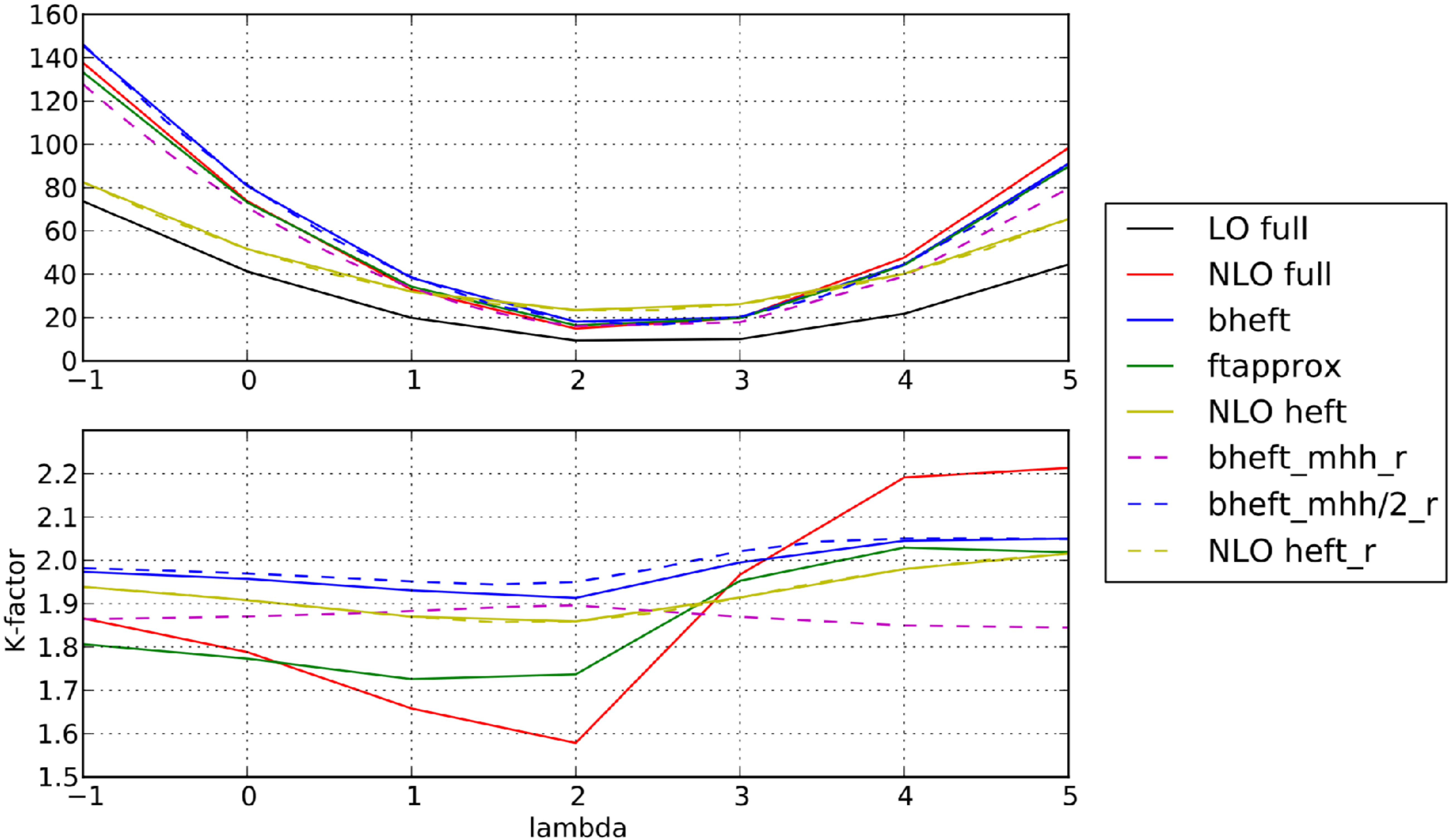

plot by Johannes Schlenk; _r: data from Ramona Gröber

NNLO_approx

$\sqrt{s}$	13 TeV	14 TeV	27 TeV	100 TeV
NLO [fb]	$27.78^{+13.8\%}_{-12.8\%}$	$32.88^{+13.5\%}_{-12.5\%}$	$127.7^{+11.5\%}_{-10.4\%}$	$1147^{+10.7\%}_{-9.9\%}$
$\text{NLO}_{\text{FTapprox}}$ [fb]	$28.91^{+15.0\%}_{-13.4\%}$	$34.25^{+14.7\%}_{-13.2\%}$	$134.1^{+12.7\%}_{-11.1\%}$	$1220^{+11.9\%}_{-10.6\%}$
$\text{NNLO}_{\text{NLO-i}}$ [fb]	$32.69^{+5.3\%}_{-7.7\%}$	$38.66^{+5.3\%}_{-7.7\%}$	$149.3^{+4.8\%}_{-6.7\%}$	$1337^{+4.1\%}_{-5.4\%}$
$\text{NNLO}_{\text{B-proj}}$ [fb]	$33.42^{+1.5\%}_{-4.8\%}$	$39.58^{+1.4\%}_{-4.7\%}$	$154.2^{+0.7\%}_{-3.8\%}$	$1406^{+0.5\%}_{-2.8\%}$
$\text{NNLO}_{\text{FTapprox}}$ [fb]	$31.05^{+2.2\%}_{-5.0\%}$	$36.69^{+2.1\%}_{-4.9\%}$	$139.9^{+1.3\%}_{-3.9\%}$	$1224^{+0.9\%}_{-3.2\%}$
M_t unc. $\text{NNLO}_{\text{FTapprox}}$	$\pm 2.6\%$	$\pm 2.7\%$	$\pm 3.4\%$	$\pm 4.6\%$
$\text{NNLO}_{\text{FTapprox}}/\text{NLO}$	1.118	1.116	1.096	1.067

considerable reduction of scale uncertainties

M_t uncertainties:
half the difference between NNLO_FTapprox and NNLO_NLO-improved

Variations of the trilinear Higgs coupling

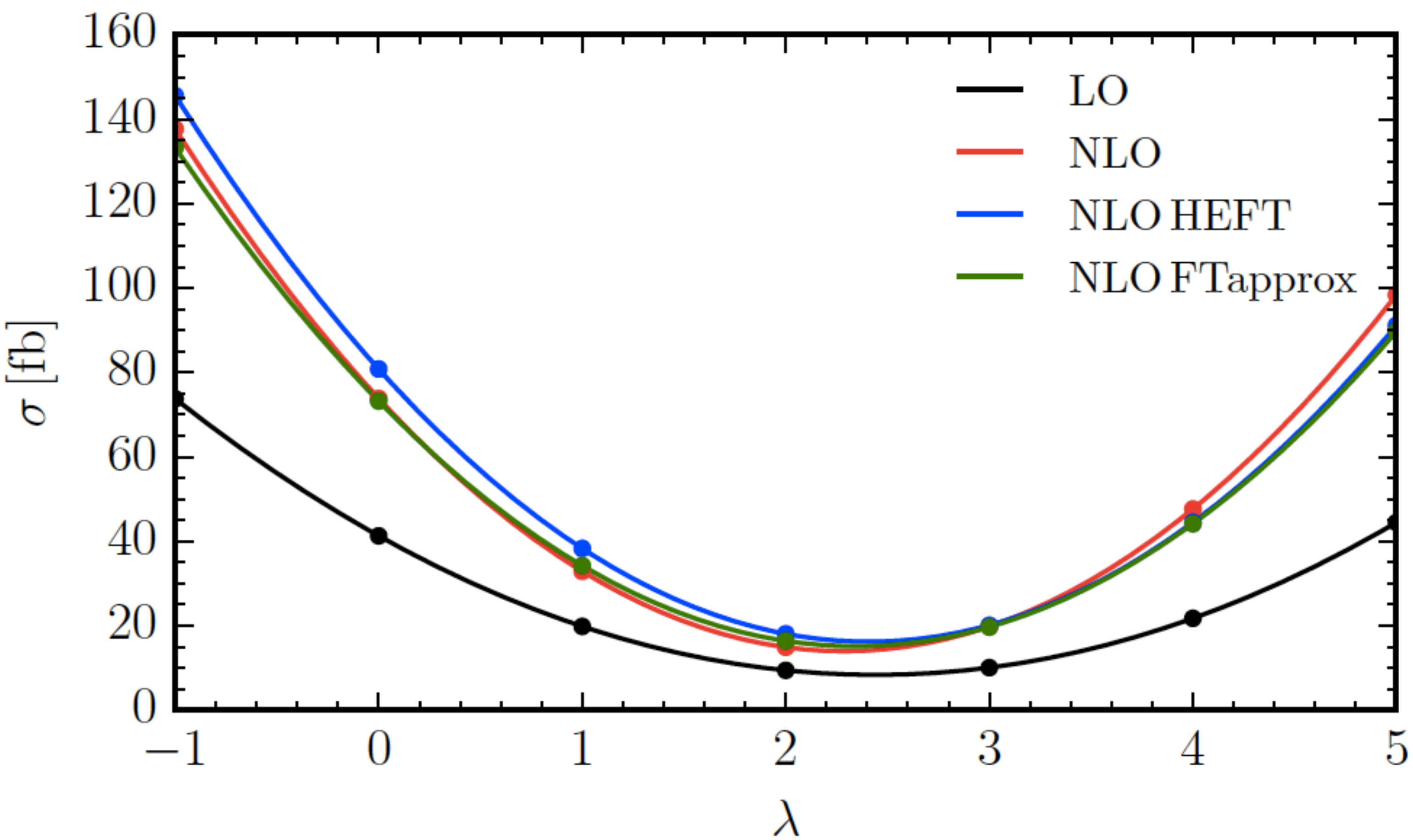

cross section is quadratic polynomial in λ

(ignoring EW corrections)

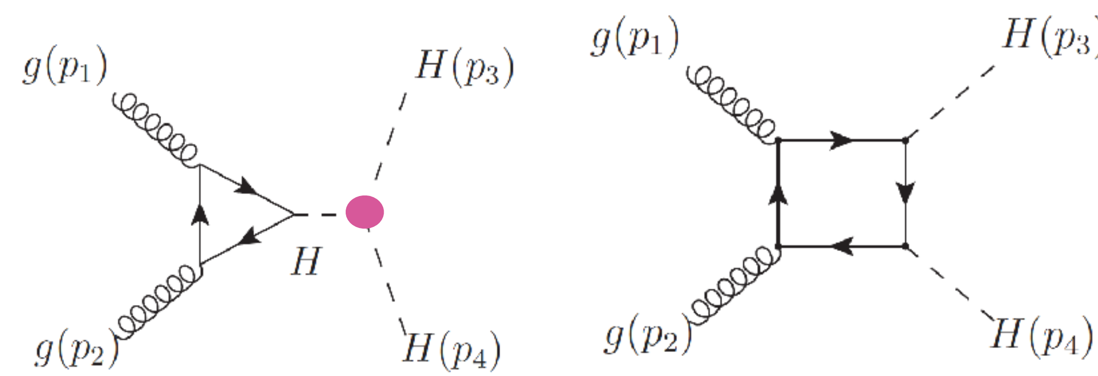

maximal destructive interference between box- and triangle-type diagrams at

$$c_{hhh} = \lambda_{\mathrm{BSM}}/\lambda_{\mathrm{SM}} \approx 2.4$$

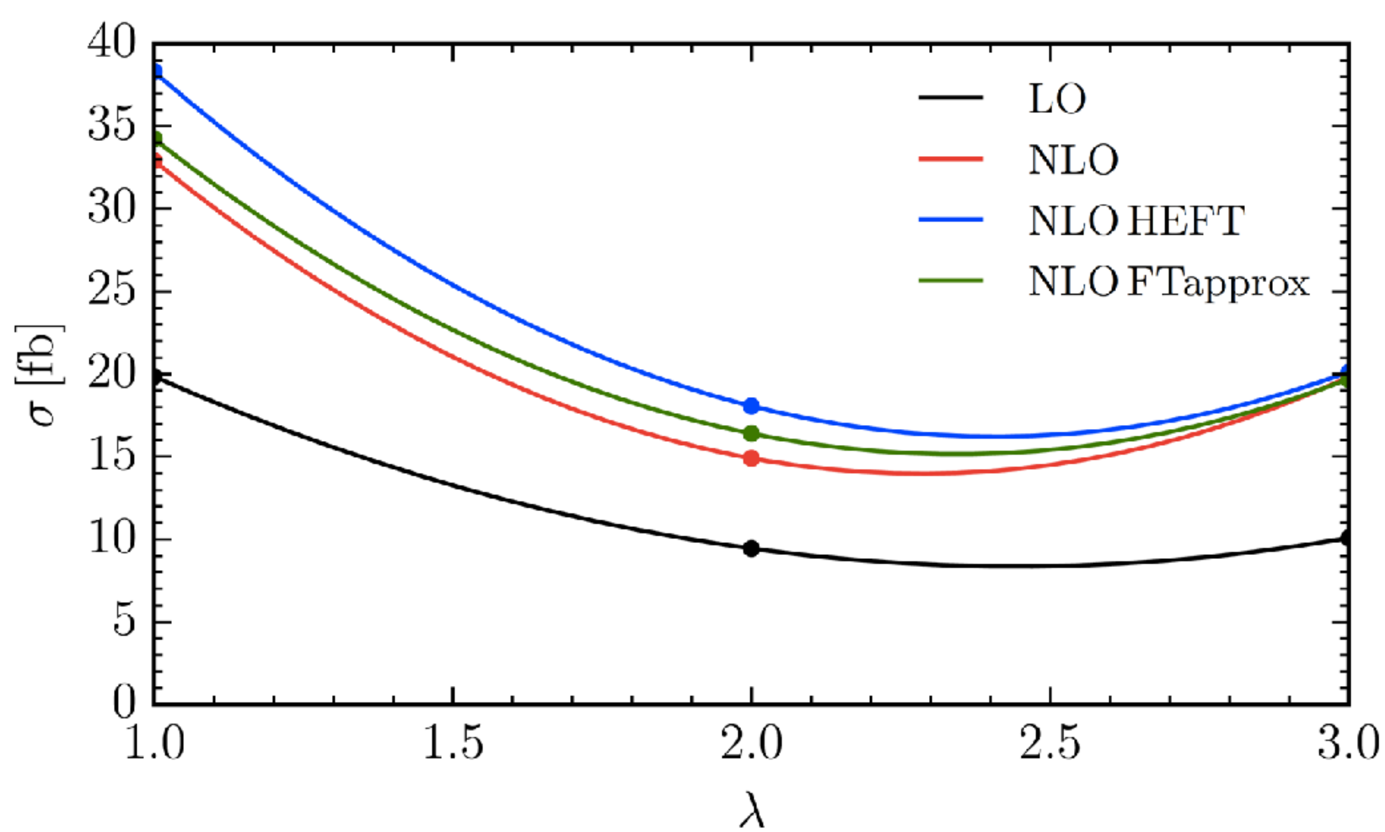

Parametrisation of the NLO cross section

$$\sigma^{\rm NLO}/\sigma^{\rm NLO}_{SM} =$$

$$A_1\, c_t^4 + A_2\, c_{tt}^2 + A_3\, c_t^2 c_{hhh}^2 + A_4\, c_{ggh}^2 c_{hhh}^2 + A_5\, c_{gghh}^2 + A_6\, c_{tt} c_t^2 + A_7\, c_t^3 c_{hhh}$$
$$+ A_8\, c_{tt} c_t\, c_{hhh} + A_9\, c_{tt} c_{ggh} c_{hhh} + A_{10}\, c_{tt} c_{gghh} + A_{11}\, c_t^2 c_{ggh} c_{hhh} + A_{12}\, c_t^2 c_{gghh}$$
$$+ A_{13}\, c_t c_{hhh}^2 c_{ggh} + A_{14}\, c_t c_{hhh} c_{gghh} + A_{15}\, c_{ggh} c_{hhh} c_{gghh}$$
$$+ A_{16}\, c_t^3 c_{ggh} + A_{17}\, c_t c_{tt} c_{ggh} + A_{18}\, c_t c_{ggh}^2 c_{hhh} + A_{19}\, c_t c_{ggh} c_{gghh}$$
$$+ A_{20}\, c_t^2 c_{ggh}^2 + A_{21}\, c_{tt} c_{ggh}^2 + A_{22}\, c_{ggh}^3 c_{hhh} + A_{23}\, c_{ggh}^2 c_{gghh}\,.$$

only present at NLO

A_i coefficients allow to reconstruct the total cross section for arbitrary values of the couplings

- also available in differential form for m_{hh} distribution
- for 13,14 and 27 TeV on https://arxiv.org/abs/1806.05162 as .csv tables

Relation to SMEFT

(restricted to Higgs sector + QCD)

SMEFT:

$$\Delta\mathcal{L}_{\rm dim6} = \frac{\bar{c}_H}{2v^2}\partial_\mu(\phi^\dagger\phi)\partial^\mu(\phi^\dagger\phi) + \frac{\bar{c}_u}{v^2}y_t(\phi^\dagger\phi\,\bar{q}_L\tilde{\phi}t_R + \text{h.c.}) - \frac{\bar{c}_6}{2v^2}\frac{m_h^2}{v^2}(\phi^\dagger\phi)^3 + \frac{\bar{c}_{ug}}{v^2}g_s(\bar{q}_L\sigma^{\mu\nu}G_{\mu\nu}\tilde{\phi}t_R + \text{h.c.}) + \frac{4\bar{c}_g}{v^2}g_s^2\phi^\dagger\phi\,G^a_{\mu\nu}G^{a\mu\nu}$$

EWChL:

$$\Delta\mathcal{L}_{d\chi\leq 4} = -m_t\left(c_t\frac{h}{v} + c_{tt}\frac{h^2}{v^2}\right)\bar{t}\,t - c_{hhh}\frac{m_h^2}{2v}h^3 + \frac{\alpha_s}{8\pi}\left(c_{ggh}\frac{h}{v} + c_{gghh}\frac{h^2}{v^2}\right)G^a_{\mu\nu}G^{a,\mu\nu}$$

relations: $c_t = 1 - \frac{\bar{c}_H}{2} - \bar{c}_u\,,\quad c_{tt} = -\frac{\bar{c}_H + 3\bar{c}_u}{2}\,,\quad c_{hhh} = 1 - \frac{3}{2}\bar{c}_H + \bar{c}_6\,,$

$$c_{ggh} = 2c_{gghh} = 128\pi^2\bar{c}_g\,.$$

non-linear EFT framework

EWChL: “loop expansion”

based on chiral dimension $d_\chi = 2L + 2$ with

$$d_\chi(A_\mu, \varphi, h) = 0, \quad d_\chi(\partial, \bar{\psi}\psi, g, y) = 1$$

expansion in canonical dimension $1/\Lambda^2$

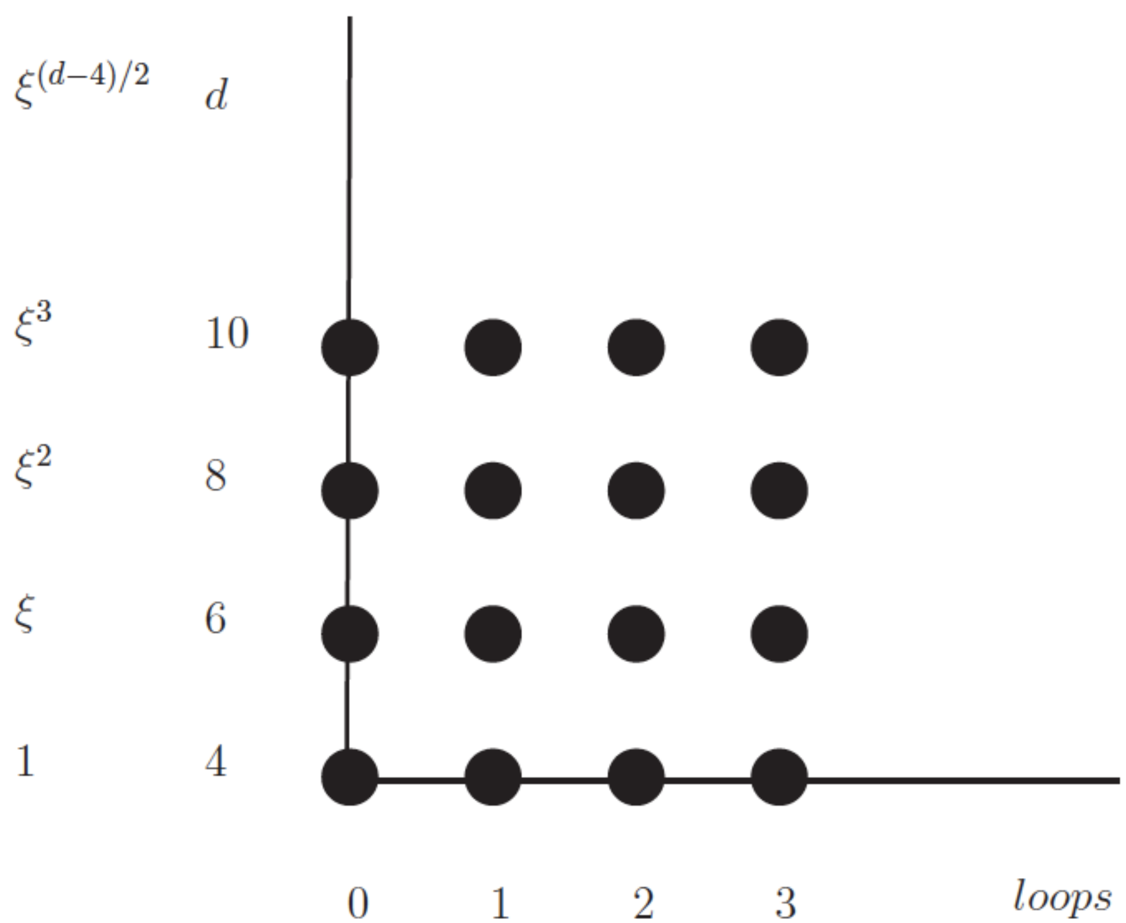

loop expansion

non-linear EFT Lagrangian

$$\mathcal{L}_2 = -\frac{1}{2}\langle G_{\mu\nu}G^{\mu\nu}\rangle - \frac{1}{2}\langle W_{\mu\nu}W^{\mu\nu}\rangle - \frac{1}{4}B_{\mu\nu}B^{\mu\nu} + \sum_{\psi=q_L,l_L,u_R,d_R,e_R} \bar{\psi} i \not{D} \psi$$
$$+\frac{v^2}{4}\langle D_\mu U^\dagger D^\mu U\rangle\,(1+F_U(h)) + \frac{1}{2}\partial_\mu h \partial^\mu h - V(h)$$
$$-v\left[\bar{q}_L\left(Y_u + \sum_{n=1}^{\infty} Y_u^{(n)}\left(\frac{h}{v}\right)^n\right) U P_+ q_R + \bar{q}_L\left(Y_d + \sum_{n=1}^{\infty} Y_d^{(n)}\left(\frac{h}{v}\right)^n\right) U P_- q_R\right.$$
$$\left.+\bar{l}_L\left(Y_e + \sum_{n=1}^{\infty} Y_e^{(n)}\left(\frac{h}{v}\right)^n\right) U P_- l_R + \text{h.c.}\right] \quad \text{(II}$$

Chromomagnetic operator

not contributing diagram types:

$y_t g_s \bar{t}_L \sigma_{\mu\nu} G^{\mu\nu} t_R$

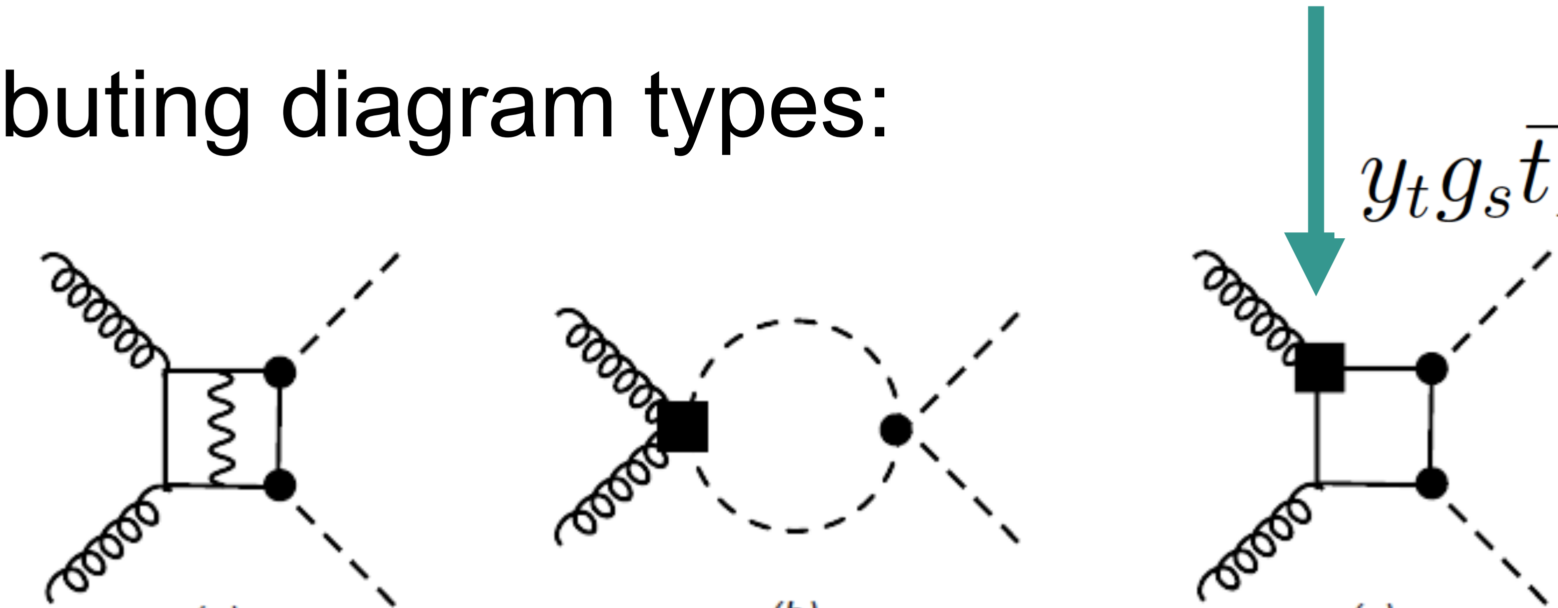

(a) (b) (c)

$g_s^2 G^a_{\mu\nu} G^{a,\mu\nu} \partial_\lambda h \partial^\lambda h$

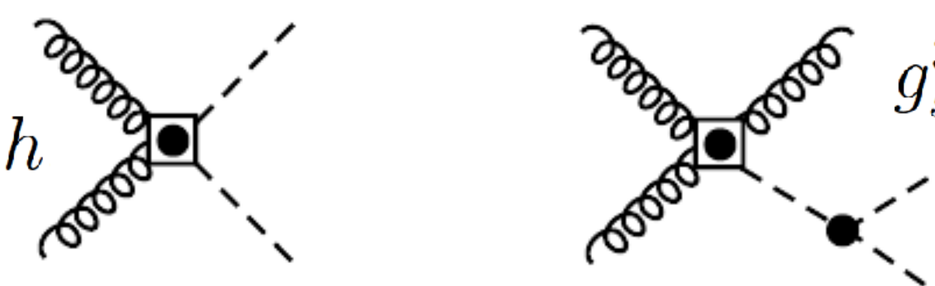

$g_s^3 f^{abc} G^a_{\mu\nu} G^{b,\nu}{}_\lambda G^{c,\lambda\mu} h$

(d) (e)

(a),(b): $d\chi = 6$ but of order $g_s^2 g_w^2$ (a), $g_s^2 c_{4h}$ (b)

(c),(d): not of order g_s^4, suppressed by $1/16\pi^2$
(operator must come from contracted loop, see hep-ph/9405214)

(e): *L*=2 interfered with real emission $\Rightarrow$ higher order

HH@NLO GoSam+Powheg

variations of top-Higgs-Yukawa coupling:

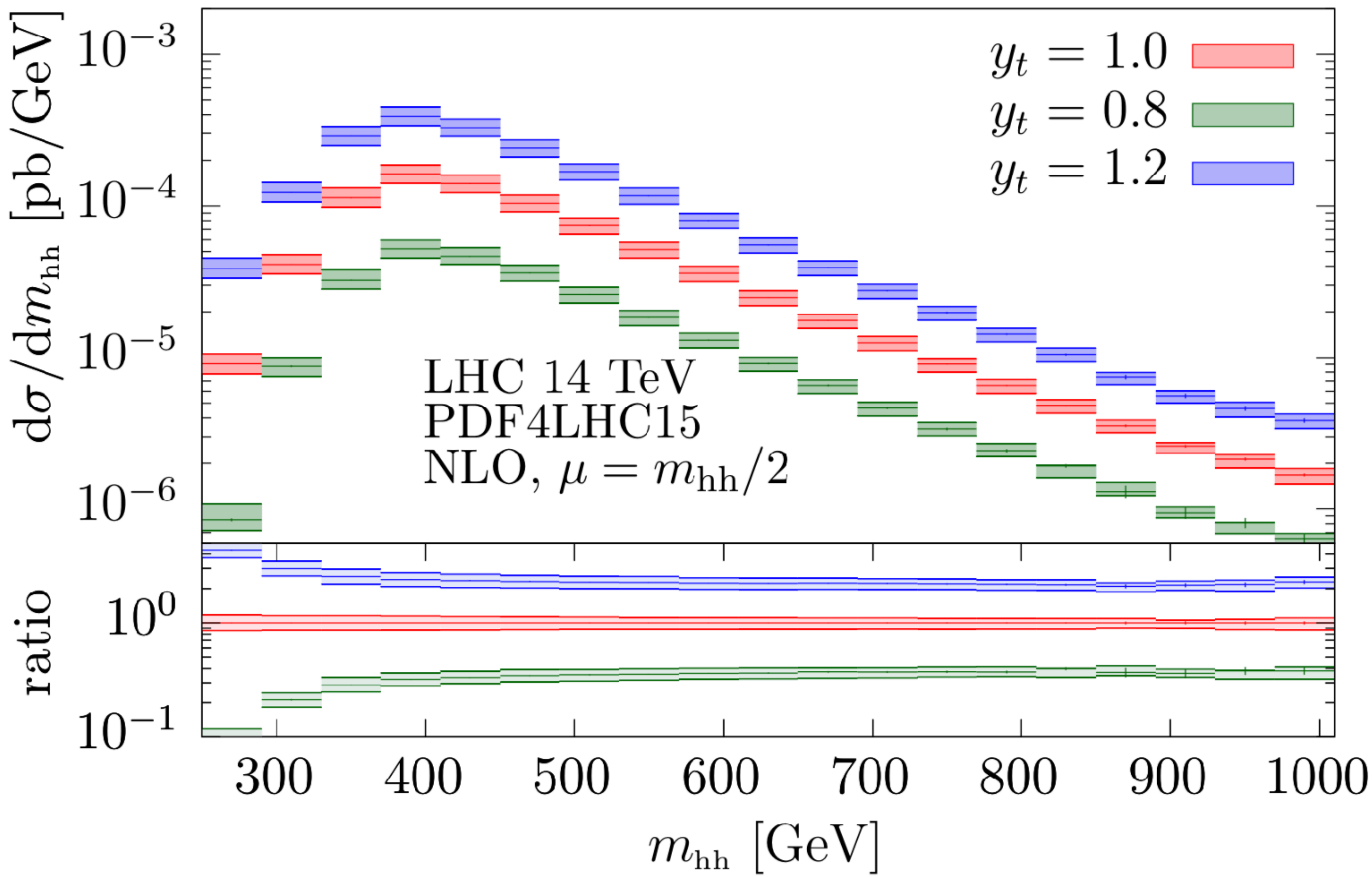

overall shift rather than shape change

HH@NLO + Parton Shower

variation of hard shower scale in Herwig7, compared to Pythia8

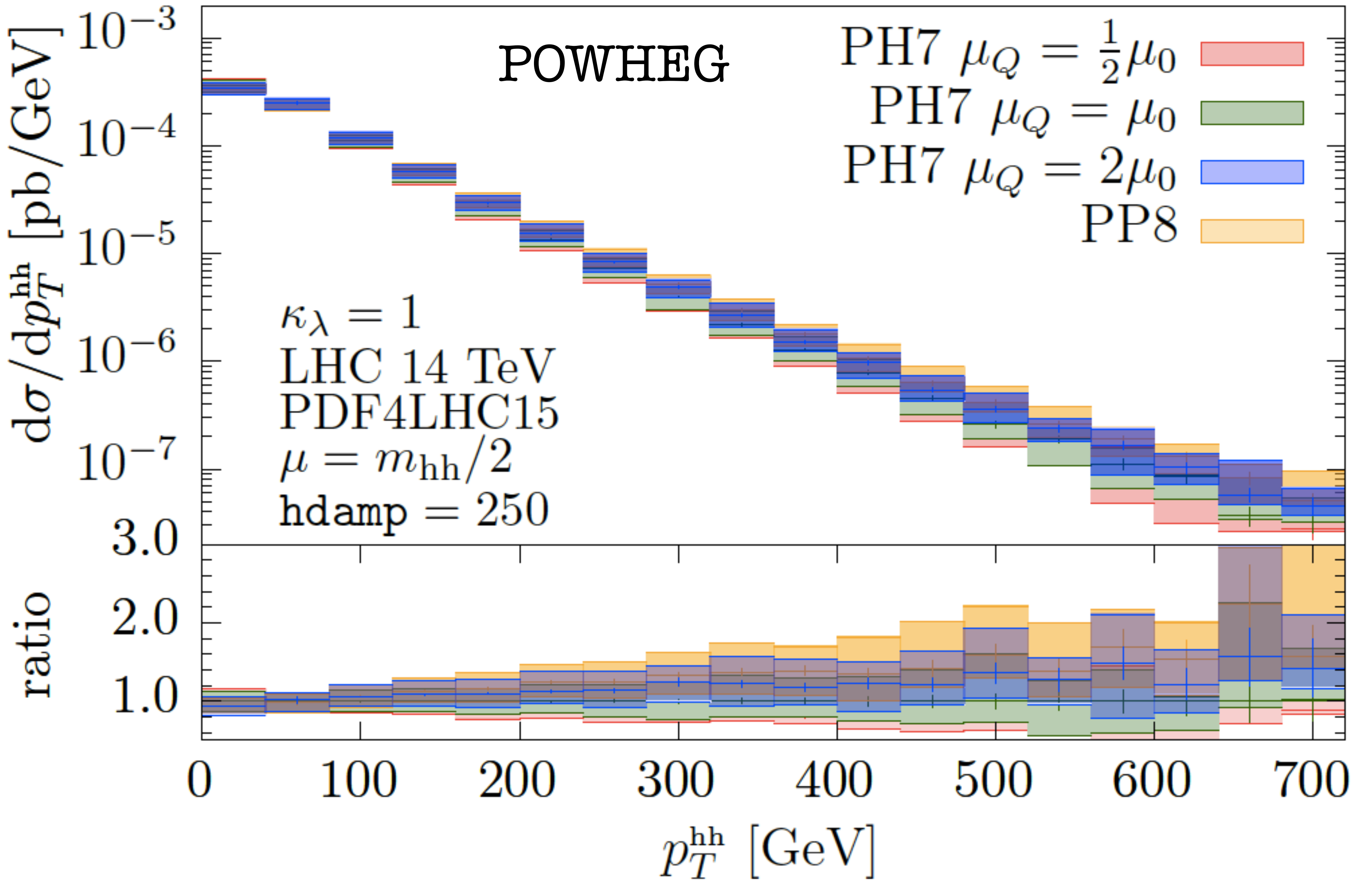

differences (almost) covered by large shower matching scale uncertainties